

Sustainable aviation fuel from forestry residue and hydrogen – a techno-economic and environmental analysis for an immediate deployment of the PBtL process in Europe

Felix Habermeyer^{*a}, Veatriki Papantoni^b, Urte Brand-Daniels^b and Ralph-Uwe Dietrich^a

Received 00th January 20xx,
Accepted 00th January 20xx

DOI: 10.1039/x0xx00000x

Sustainable aviation fuels offer the opportunity to reduce the climate impact of air transport while avoiding a complete overhaul of the existing fleet. For Europe, the domestic production of sustainable aviation fuel would even lead to a reduced dependency on energy imports. Biomass-based fuel production in Europe is limited by the availability of sustainable biomass. This limitation can be alleviated by the Power and Biomass to Liquid (PBtL) process, which attains near full biogenic carbon conversion to Fischer-Tropsch fuel by the addition of electrolytic hydrogen. This study evaluates the economic feasibility and environmental impact of the sustainable aviation fuel production from European forest residue based on a region-specific analysis. As of 2020, only a few sweet spots, such as Norway or Sweden, could serve as production sites for sustainable PBtL fuel when the electrical energy for the electrolysis is supplied by the national grid. The grid mix for many other countries is too carbon intensive to justify producing PBtL fuel there. Yet, with the direct usage of renewable electricity sources, a fuel output of 25 Mt/a can be reached assuming 33 % of all forest residue can be used for fuel production. Under these conditions, the EU goal of providing 32 % of the total aviation fuel demand with sustainable aviation fuel in 2040 could be met.

1. Introduction

The European aviation industry faces two challenges today. First, as a net contributor of 3.8 % to the total European CO₂ emissions¹⁰, the aviation industry is poised to reduce its carbon emissions to net-zero by 2050¹³. Sustainable aviation fuel (SAF) offers an immediate solution for emission reduction that does not require a complete technology overhaul of the existing fleet by switching to alternative energy carriers or propulsion systems¹⁷ as with hydrogen or battery-electric aircrafts. Accordingly, the European Union aims to increase the SAF share in the fuel mix to 63 %_{vol.} by 2050 with its ReFuelEU Aviation initiative²². Secondly, the aviation industry is faced with the uncertainty related to energy imports. As currently seen with gas imports²⁴ or the oil crises of the 1970s, energy imports have an inherent default risk.

The Power and Biomass to Liquid (PBtL) process offers a solution for both challenges, as low greenhouse gas (GHG) SAF can be produced within Europe. The PBtL process converts biomass feedstock via gasification to syngas. With the addition of electrolytic hydrogen, syngas reacts to hydrocarbon chains via the Fischer-Tropsch (FT) route. The product is then refined

to FT synthetic paraffinic kerosene (FT-SPK), which is certified as a 50 % drop-in fuel¹¹. PBtL is not the only route to convert biomass to SAF. Alcohol to jet (AtJ), the synthesised iso-paraffine (SIP), and other Fischer-Tropsch routes without the addition of electrolytic hydrogen (Biomass to Liquid - BtL⁹) are also certified as drop-in fuels^{30, 31}. The PBtL process stands out from its alternatives due to its high carbon conversion. In general, SAF production processes convert a carbon source with low energy content (e.g. CO₂ 0 MJ_{LHV}/kg or dry biomass 19 MJ_{LHV}/kg) to a highly energy-dense fuel (43 MJ_{LHV}/kg). A full conversion of the carbon is only possible with an additional energy input³. The energy input via electrolytic hydrogen addition in the PBtL process leads to a higher carbon conversion compared to the BtL process. However, the additional product output has to be weighed against additional cost and global warming potential (GWP) for the hydrogen production.

To evaluate whether the PBtL process is a suitable solution for the production of SAF in Europe, three criteria have to be met. First, the European aviation sector will have an annual estimated fuel demand of 63 Mt/a by 2030²¹. Can the PBtL process cover a significant amount of this SAF demand given the limited biomass feedstock in Europe? Secondly, the environmental impact of the production chain has to be analysed. GHG emissions of sustainable fuel should be reduced by 65 % compared to fossil fuel, i.e. less than 32.9 g_{CO₂,eq}/MJ_{fuel}, as defined in the RED II directive¹¹. Third, a cost analysis has to be conducted to understand whether the fuel can be produced at a reasonably low price.

^a Institute of Engineering Thermodynamics, German Aerospace Centre (DLR), 70569 Stuttgart, Germany.

^b Institute of Networked Energy Systems, German Aerospace Centre (DLR), 26129 Oldenburg, Germany.

† Electronic Supplementary Information (ESI) available: [details of any supplementary information available should be included here]. See DOI: 10.1039/x0xx00000x

Tab. 1. Studies on the production of SAF from biomass and electrolytic hydrogen.

Study	Study type	Main finding	Reference year	Geographical scope	Key assumptions	Plant size
Hillestad et al. ³	TEA	NPC 1.7 \$/l	2014	Norway	50 \$/MWh (grid)	435 MW _{th} biomass input
Albrecht et al. ⁹	TEA	NPC 2.15 €/l	2014	Germany	105 €/MWh (grid)	240 kt/a product output
Isaacs et al. ¹²	TEA, GWP focused LCA	Grid: NPC ₂₀₁₆ 1.84 \$/l, GWP ₂₀₁₆ 187 g _{CO2,e} /MJ _{fuel}	2016, 2030 and 2050	USA	67.3 \$/MWh (grid)	1000 t _{dry} /d (~200 MW _{th,dry})
Bernical et al. ¹⁶	TEA, GWP focused LCA	NPC 1.5 €/l GWP 41 g _{CO2,e} /kWh _{fuel}	2011	France	70 €/MWh 55 g _{CO2,e} /kWh _{grid} (grid)	500 MW _{th} biomass input
O'Malley et al. ²¹	Fuel potential	0.22 Mt _{SAF} /a from forest residue (fr)	2030	EU	BtL route (5.1 Mt _{fr} /a, 39 % utilization, 0.22 g _{FT} /g _{fr} , 0.5 g _{SAF} /g _{fr})	
Prussi et al. ²³	Fuel potential	Enough biomass potential to completely cover SAF demand	2019	EU28	BtL route	

1.1. Literature review

An overview of studies related to SAF production via the PBtL process shown in Tab. 1. The PBtL process has been the subject of several techno-economic analyses (TEA). Hillestad et al. find net production costs (NPC) of 1.7 \$₂₀₁₇/l for a PBtL process with 435 MW_{th} biomass input assuming an electricity price of 50 \$/MWh³. Thereby, near full carbon recycling leads to a carbon efficiency of 91 %. Albrecht et al. estimate production costs of 2.15 €₂₀₁₄/l_{GasolineEquivalent} at an electricity price of 105 €/MWh⁹. The simulated PBtL plant with an output of 240 kt/year has a carbon efficiency of 97.7 %. Isaacs et al. estimate local production costs for PBtL plants in the eastern part of the USA based on local biomass prices and PV and wind availability¹². For every location, an off-grid electrolysis and hydrogen storage system is designed to produce a constant hydrogen stream at minimal cost. For the year 2030, the most inexpensive product quartile has a minimum selling price of 2.40 \$₂₀₃₀/l for systems operated with PV and wind input. Studies regarding the environmental impact assessment of synthetic fuels focus on jet fuel via gasification of forestry residues and FT-synthesis (BtL pathway)^{35, 36} or via water electrolysis, direct air capture, and FT-synthesis (PTL pathway)^{37, 38}. Bernical et al. investigate the combination of the BtL process with additional hydrogen sources (namely high-temperature steam and alkaline electrolysis) in order to benefit from the higher carbon conversion rate of such a hybrid process¹⁶. Apart from a techno-economic analysis, they also evaluate the GHG emissions of the hybrid pathway and

demonstrate that it can only result in fuels compatible with EU requirements when electricity sources with very low fossil carbon intensity are used for electrolysis. Isaacs et al. also conduct an LCA of the PBtL pathway in the USA for various biomass feedstocks (corn stover, switchgrass or willow) accounting for regional availability and compare it to the PtL and BtL pathways¹². The study focuses on the impact of fuel production on climate change in terms of GWP and confirms the high sensitivity of the result to the electricity's emission intensity.

O'Malley et al. estimate the SAF production from forest residue via the BtL route to be 0.22 Mt/a in Europe by 2030²¹. The authors account for feedstock availability, sustainable harvesting limits, utilisation competition for those materials, and SAF conversion yields. Yet, only the conversion via the BtL route is considered. This inevitably leads to lower SAF yields compared with PBtL. Furthermore, Prussi et al. claim that GHG neutrality in the European aviation industry can be achieved with the FT BtL route²³. However, this statement is based on rough calculations assuming all possible feedstock, biomass from forestry and agriculture as well as municipal waste, is used for the production of aviation fuel²³. Throughout literature no study on the SAF production potential of the PBtL process in Europe was found.

The aim of this study is to assess the economic feasibility and ecological impact of sustainable aviation fuel production via the PBtL process in Europe. The novelty in this approach lies in the combination of fuel production potential estimation, LCA and



Fig. 1. Power Biomass to Liquid (PBtL) flowsheet showing all major process components.

TEA, which take the local European boundary conditions into consideration. The analysis is based on a flowsheet simulation of a fixed size PBtL plant implemented in Aspen Plus[®]. To account for the production conditions within Europe, such as biomass and electricity price or GHG footprint of the local electricity production, an individual TEA and GHG emission calculation is conducted for around 300 European NUTS2 regions. Grid power, PV and wind energy are considered as energy sources for the PBtL process in separate scenarios. With this analysis, this study gives a unique insight into the PBtL process' SAF production volume, cost and GWP within Europe, as so far only studies for single locations have been published. A similar region-specific analysis has been conducted for the USA. However, this study also omits discussing the amount of SAF that can be produced within the analysed region.

2. Methodology

2.1. Process description

Fig. 1 depicts the process flowsheet including all selected technology options. The base case is simulated with a biomass input of 400 MW_{th}. This has been shown to be a feasible size for processes with forest residue as feedstock³⁹. It might be beneficial for future individual production sites, to adapt the plant size to the local availability of unused biomass and renewable electricity. Yet, for this calculation the size is kept constant.

This study focuses on forest residues omitting agricultural residues or municipal and industrial waste, which could also serve as feedstock for an FT process²¹. Agricultural residues, especially, have a larger potential compared to forest

residues^{21, 40}. Yet, syngas production from forest residue appears to be less energy- and capital-intensive, as other feedstocks tend to have a higher contaminant content⁴¹.

A circulating fluidised bed (CFB) gasifier is selected for its low capital cost, broad spectrum of biomass feedstock and low oxygen demand^{42, 43}. The CFB gasifier uses CO₂ recycled from the syngas cleaning section as a dilution medium for the oxygen provided by the electrolyser. This type of gasification can be referred to as CO₂ gasification⁴⁴. Ash from the gasifier is removed via a filter unit.

Biomass drying is accomplished with a belt dryer using air as drying medium. Air is used here instead of steam because the PBtL process is exothermic. Thus, the low temperature heat for air drying can be supplied by the process itself.

The syngas' tar concentration is reduced with a catalytic tar reformer. The reformation reaction decomposes large tar components into light gases^{41, 45}. Recycled CO₂ is used as a dilution medium for the reformer oxygen feed as well. Additionally, this reactor partially reforms methane and ammonia. Compared to high temperature cracking, catalytic tar cracking requires less oxygen to reach its lower operation temperature⁴². Thereby, more H₂ and CO can be retained.

The removal of syngas contaminants, which can act as catalyst poison on the Fischer-Tropsch catalyst, is accomplished with cold gas cleaning steps. A heat recovery steam generation unit (HRSG) makes use of the syngas heat before feeding it into a water scrubber. The scrubber reduces the water content along with other gas contaminants such as ammonia⁴². CO₂ and H₂S are removed in a Selexol scrubber⁴⁶. Selexol was shown to have the lowest energy requirement for CO₂ removal compared to alternative removal technologies⁴⁶. Before entering the Selexol

scrubber, the syngas stream is compressed. Higher pressure levels are also beneficial for ab- and adsorption processes in the subsequent cleaning steps. Finally, trace contaminants such as alkali compounds are removed in a guard bed⁴².

The slurry bubble column (SBCR) is chosen as the Fischer-Tropsch reactor for its low investment costs at large scale⁴⁷ compared to micro-channel reactors and its relatively high CO conversion per pass compared to fixed bed reactors⁴⁸.

Hydrogen and oxygen for the process are provided by an alkaline electrolysis (AEL) system, as the technology has the lowest current investment costs and the highest technological maturity³⁴. AEL systems are even capable of operating with a flexible load due to their nominal load ramp speed of around 2 %/s⁴⁹. In addition, no rare material is needed for the AEL production as opposed to the PEM technology, whose iridium demand might prove to be a bottleneck in the future⁵⁰.

In summary, that process was tested and validated in many research and demonstration projects in the past^{51, 52} and still lacks full-size proof of operation. However, current engineering knowledge provides enough confidence for a simulation of a full-size plant.

2.2. Process model

The process model is implemented in the commercial simulation software Aspen Plus® (V10). For the Aspen Plus® flowsheet, the Soave-Redlich-Kwong equation of state is used⁵, which is the recommended property method for hydrocarbon processes⁵³. In the following sections, crucial modelling

parameters are discussed in detail. Further assumptions can be found in the electronic supplementary information (ESI). A more detailed description of the modelling assumptions can be found in Habermeyer et al.⁴.

2.2.1. Feedstock. As feedstock for the process, forest residue is chosen. The corresponding composition and higher heating value (HHV) are listed in Tab. 2. The initial moisture content before drying is assumed to be 50 wt. %⁵. Before introducing biomass to the gasifier, the moisture content is decreased to 12 wt. %⁵ in the belt dryer.

2.2.2. Gasification and reformer. The circulating fluidised bed gasifier is operated at 850 °C and 4 bar^{4, 5}. The main syngas components are brought into chemical equilibrium at 900 °C using a RGibbs reactor. The yield functions for all other gasification products can be found in the ESI. The oxygen input is iterated in order to attain a heat loss of 1 % of the biomass feed's LHV. Recycled CO₂ is used in gasifier and autothermal reformer as dilution medium, whereby the gasifier has an equal feed mass ratio of oxygen to CO₂. All remaining CO₂ is recycled to the reformer, which is simulated as an adiabatic equilibrium stage at 850 °C⁴. For this stage a CH₄ conversion of 35 % is assumed⁴.

2.2.3. Fischer-Tropsch. The Fischer-Tropsch SBCR reactor is simulated with the kinetic reaction model developed by Todic et al.⁵⁴. The corresponding implementation in a FORTRAN subroutine is documented in Habermeyer et al.⁴. The CO conversion of 55 %⁴⁸ at a fixed operation point of 220 °C and 25 bar is attained by iterating the catalyst mass in the FT reactor. In this study, the Fischer-Tropsch fraction C₅₊ is considered as the final product of the process and subsequently regarded as SAF. Additional cost and conversion losses in the refining process are therefore not within the scope of this study. The pressure for the FT reactor is selected to maximise the selectivity for the product fraction C₅₊ within the model's validity boundaries. The FT temperature of 220 °C is assumed to simulate a realistic product output. During operation, the FT reactor temperature is continually increased to counteract reversible catalyst degradation, thereby keeping the CO conversion constant. Therefore, selecting a temperature in the middle of the model's valid range (205 – 230 °C) reflects a typical reactor operation.

2.2.4. Electrolyser. The AEL is operated at the FT pressure level of 25 bar, whereby the H₂ output is iterated to achieve an H₂/CO ratio in the FT feed. The system efficiency is assumed to be 70.8 %_{HHV}³⁴.

Tab. 2. Forest residue properties.³⁰

Proximate analysis	wt. % dry basis
Fixed carbon	25.3
Volatile matter	70.8
Ash	3.9
Ultimate analysis,	wt. % dry basis
Ash	3.9
C	53.2
H	5.5
N	0.3
Cl	0
S	0.04
O (difference)	37.06
Other properties	
HHV, MJ/kg	20.67
LHV, MJ/kg	19.34
Initial moisture content, wt. %	50

Tab. 3. Equipment cost functions.

Unit	E_{ref}	Currency	S_{ref}	Unit	k	Year	Source	FCI method ^d
Belt dryer and feedstock handling	24.8	M€	10.22	Evaporated water, kg/s	0.7	2019	4	5
Ceramic hot gas filter	6.8	M€	1.466	Syngas input, kmol/s	0.67	2010	5	3
Guard bed	6	M€	260	Syngas. MW_{th}	0.85	2010	5	4
Selexol scrubber	54.1	M\$	9909	CO ₂ feed, kmol/h	0.7	2001	18	5
Water scrubber	5.2	M€	1.446	Syngas input, kmol/s	0.67	2010	5	3
Pressurised O ₂ CFB gasifier	37.7	M€	37.7	Dry biomass, kg/s	0.75	2010	5	4
HRSG	6	M€	43.6	Transferred heat, [MW]	0.8	2010	5	3
Syngas compressor	5	M€	10	Compression work, MW_e	0.67	2010	5	3
CO ₂ compressor	5	M€	10	Compression work, MW_e	0.67	2010	5	3
Catalytic reformer	21.8	M€	2.037	Syngas, kmol/s	0.67	2010	5	3
Gas/liquid separator ^a	0.09	M€	10	Unit length, m	0.79	2014	26	1
Fischer-Tropsch SBCR ^b	2.025	M\$	341.3	Reactor volume, m ³	0.67	1998	33	1
AEL ^c	1	M€	1	Electrical power input, MW_e	0.8	2019	34	5
Refrigeration System	1976	\$	1	Refrigeration capacity, kW	0.67	2002	26	1

^a Cost data for storage vessels were used. The cost function has three input parameters (vessel length, vessel diameter, pressure). The stated cost function is an example based on a horizontal storage vessel with a diameter of 2 m at pressure levels up to 10 bar⁹.

^b The reactor volume V is calculated assuming a catalyst loading of 140 kg/m³³³. The specific cost for the cobalt catalyst (cobalt + support) is calculated with 33.07 \$₂₀₀₇/kg²⁰.

^c It is assumed that 80 % of the equipment cost can be attributed to the AEL stack and 20 % to the peripheral equipment. For the FCI estimation, stack costs are assumed to be turn key (method 5). 2 % of the stack FCI has to be spent annually on maintenance. The peripheral equipment FCI is estimated with method 2. The costing method is based on a correspondence with an AEL supplier.

^d Fixed capital investment FCI calculation methods described in the ESI

2.2.5. Heat integration. The heat integration procedure determines the quantity of utilities supplied to or produced in the process. Net cooling demand and net heat generation are calculated in DLR's software tool TEPET by balancing the process' heat streams. The exact heat integration algorithm can be taken from Maier et al.⁵⁵. In this study, it is assumed that steam can be sold at three pressure levels: 10 bar at 183 °C (low pressure steam, LPS), 20 bar at 215 °C (medium pressure steam, MPS) and 35.5 bar at 245 °C (high pressure steam, HPS). Heat below the temperature of 183 °C, that is not used to heat up cold process streams, has to be cooled using cooling water at 25 °C. For the FT product separation at a temperature of 0 °C a refrigeration cycle is considered.

2.3. Technical process evaluation

Mass and energy balances are retrieved from the Aspen Plus[®] process simulation. Based on the resulting balances, the following four process performance indicators can be calculated. The carbon conversion denotes the percentage of biomass carbon that can be transformed to FT product.

$$X_C = \frac{\dot{m}_{C,prod}}{\dot{m}_{C,biom}} \quad \#(1)$$

The biomass conversion sets the total product mass in relation to the wet biomass input. As biomass consists of components that cannot be converted to FT product, the biomass conversion value is inevitably lower than 100 %.

$$X_{biom} = \frac{\dot{m}_{prod}}{\dot{m}_{biom,wet}} \quad \#(2)$$

The energy fraction converted to product from biomass and electrical power input is represented by fuel efficiency.

$$\eta_{fuel} = \frac{\dot{m}_{prod}LHV_{prod}}{\dot{m}_{biom}LHV_{biom} + P_{el,input}} \quad \#(3)$$

The process efficiency additionally includes by-products, in this case steam, at different pressure levels. Here, only the evaporation enthalpy ΔH_v is considered.

$$\eta_{process} = \frac{\dot{m}_{prod}LHV_{prod} + \sum \dot{m}_{by-prod}\Delta H_v}{\dot{m}_{biom}LHV_{biom} + P_{el,input}} \quad \#(4)$$

2.4. Production cost estimation

The cost estimation methodology used in this study is described in Peters et al.²⁶. This methodology can be considered a current standard methodology on this field and is therefore used in many recent techno-economic studies⁵⁶⁻⁵⁸. The plant's net production cost (NPC) is comprised of the annuity for the capital expenditure (CAPEX), the direct operation expenditure (OPEX), including feedstock and utility cost, and the indirect operation cost, accounting for cost factors like insurance. The cost estimation is conducted with the software tool TEPET, as described by Albrecht et al.⁹ and Maier et al.⁵⁵.

The capital expenditure is estimated based on equipment cost as well as indirect capital cost, such as the cost of installation. The equipment cost functions used for this study are given in Tab. 3. Here, a unit's equipment cost E follows from cost (E_{ref}) and size (S_{ref}) of a reference unit as a function of the unit's size S and a scaling exponent k . The cost estimation is conducted for the year 2020. The CEPCI index method is used to account for inflation when cost functions from older sources are used²⁶. Further, the exchange rate to Euro is considered by using the yearly average exchange rate⁵⁹.

$$E = E_{ref} \left(\frac{S}{S_{ref}} \right)^k \quad \#(5)$$

Indirect capital costs are estimated by multiplying the equipment costs with the factors defined in the corresponding FCI method. These factors defined in Tab. 3 can be found in the ESI. The sum of direct and indirect investments is referred to as fixed capital investment (FCI). The plant annuity, which accounts for the plant's depreciation, is then calculated assuming the plant can be operated for 20 years with an interest rate of 7 %⁵⁵.

Direct operation costs are calculated with the prices given in Tab. 4. For the base case, typical electricity and biomass prices for Finland⁵ are considered. Indirect operation costs, such as maintenance and insurance, are estimated with the factors given in the ESI. The cost of operating supervision for example is estimated as 15 % of the operating labour. Here, the operating labour for the plant is estimated as 80 000 h/a with average labour costs of 43.14 €/h⁹.

Tab. 4. Base case utility prices.

Utility	Prices	Source
Wet biomass	42.232 €/t _{50%moist.}	5
Electricity	50.4 €/MWh	5
Demineralised water for electrolysis	2 €/m ³	14
Cooling water	0.005 €/l	9
FT catalyst ^a	33 €/kg	20
Selexol ^b	4.395 €/kg	9
Waste water	0.918 €/m ³	26
HPS	17.706 €/t	27
MPS	16.057 €/t	27
LPS	13.142 €/t	27

^a catalyst lifetime 2 years³²

^b Selexol makeup 0.00018 kg_{makeup}/kmol_{syngas}⁹

2.5. Environmental impact assessment

Various environmental analysis methods have been developed over time, including procedural ones, such as Environmental Impact Assessment (EIA) or Strategic Impact Assessment (SIA), and analytical ones, such as Life Cycle Assessment, Material Flow Analysis and Environmental Risk Assessment⁶⁰. The procedural methods EIA and SIA are usually applied to large projects in order to assist authorities or companies in their decision-making process. Analytical methods are more common in the assessment of products. LCA is used for environmental assessment in this study, as it allows to quantify the environmental impacts of a product, in this case sustainable aviation fuel, in different categories and provides insights into the contributions of single life cycle stages and processes to the overall impact.

According to the guidelines introduced in DIN EN 14040/44⁶¹ the LCA consists of four phases being: the goal and scope definition of the analysis, the inventory analysis, where the data

describing the inputs and outputs of the product system is collected, the impact assessment, where the impact of the inventory processes is evaluated in specific environmental impact categories, and the interpretation that reflects the results of the analysis considering the defined goal and scope.

In order to calculate the environmental impacts of the PBTL production, an attributional LCA is conducted following the principles introduced in DIN EN 14040/44⁶¹ using the open-source software brightway2⁶². The process depicted in the PBTL process flowsheet in Fig. 1 as well as the collection of the biomass feedstock, transport of the biomass to the plant, and construction of the plant are included within the system boundaries. Environmental impacts of refining the FT product are not considered in this study. This system definition corresponds to the one used for the economic assessment.

The functional unit ("*quantified performance of a product system for use as a reference unit*"⁶¹) is 1 MJ_{LHV} of produced FT product following the described PBTL pathway in Europe in the timeframe from 2020 to 2050.

The Aspen Plus[®] simulation of the PBTL process, as described in section 2.1, and the corresponding mass and energy balance data (see ESI) serve as basis for the life cycle inventory (LCI). This data is used to model the system processes (activities) in brightway2 using the ecoinvent life cycle inventory database v3.7.1 (system model "allocation, cut-off by classification")⁶³ as a background database.

Regarding the life cycle inventory for the PBTL process, the following assumptions are made: The forestry residue feedstock is modelled by adapting the ecoinvent process "market for wood chips, wet, measured as dry mass, Europe without Switzerland" to exclude wood chips coming from sawmilling plants and the respective transport. This adaptation is done as it is assumed that all biomass for the PBTL production consists of primary residues harvested directly in forests and does not include secondary residues. Other variabilities in forestry practices, wood characteristics or carbon uptake by different tree species (e.g., spruce vs. oak) are not considered due to the lack of data. The harvested wood chips are assumed to be transported by trucks over a distance of 100 km, corresponding to a typical transport radius (see section 2.7.1). Regarding the PBTL production, the material compositions for the reformer catalyst and the active material of the guard bed are based on data from the FLEXCHX project⁶⁴, while the FT catalyst data is based on the publication by Todić et al.⁵⁴. The amounts of catalysts (also considering their lifetimes) are derived from the Aspen Plus[®] model and data from the FLEXCHX project. A general landfilling process from the ecoinvent database is used for the disposal of the spent catalysts after their end of life due to the lack of more specific data. The material composition for Selexol is based on Schakel et al.⁶⁵. Regarding the PBTL plant construction, the inventory data for the construction of the electrolyser is based on Wulf and Kaltschmitt⁶⁶ and Delpierre et al.⁶⁷, while the construction of the other components of the PBTL plant is based on the ecoinvent process "synthetic gas factory construction, CH" that describes a biomass gasification plant in Switzerland, and the process "petroleum refinery construction, Europe" as a proxy

for the syngas cleaning and FT-reactor facilities. All mentioned plant construction inventories are scaled to match the requirements of the studied PBtL plant. As to the output flows of the PBtL production, the resulting wood ash is assumed to be treated using the European “market for wood ash mixture, pure” process ofecoinvent. All other output flows (except for the by-product steam) are assumed to be emitted to the environment (air or water) without further treatment in order to quantify the burdens for the environment without alteration. Treatment of the resulting wastewater in a suitably designed treatment plant would be possible, however it is not modelled here due to the lack of more specific data. More details on the LCI can be found in the ESI.

The economic assessment considers the excess steam produced by the PBtL plant as a by-product that creates revenue (see section 2.2.5). Thus, the system is assumed to have two products: the FT product and steam. In order to solve this multifunctionality and for consistency with the economic assessment, an economic allocation using the prices employed in the economic assessment is applied.

The impact categories chosen for the LCA are listed in the ESI. The corresponding LCA methods follow the methodology and characterisation factors recommended by the International Reference Life Cycle Data System (ILCD 2.0 2018 / EF 2.0). According to the ILCD recommendations, the results of the impact categories ecotoxicity (freshwater), land use, water scarcity, resource use/minerals and metals, and resource use/energy carriers need to be viewed with caution⁶⁸.

In order to better understand the impact of each step along the process chain, the PBtL production process is subdivided into partial processes, such as electricity, biomass transport, etc. The corresponding LCIs are provided in the ESI. These partial processes form the basis of a contribution analysis using the functions of the bw2calc package of brightway2.

2.6. Biomass potential analysis

One goal of this study is to evaluate the potential for fuel production via the PBtL pathway from European forest residue. For the purposes of this analysis, the ENSPRESO (ENergy System Potentials for Renewable Energy SOurces) dataset^{69, 70} is used. It is an open-access dataset containing renewable energy potentials with different levels of geographic disaggregation (NUTSO and NUTS2 levels) for the period between 2010 and 2050 for the EU-28 countries (and some additional European countries).

Three scenarios (High, Medium and Low bioenergy availability) with different assumptions regarding land use, forestry practices, and sustainability limitations are defined in the ENSPRESO dataset. The scenarios also include assumptions regarding the competition from non-energy sectors (e.g., material use, bio-based products) and consider this in the resulting biomass potentials⁶⁹. For the purposes of this analysis only the Medium and Low bioenergy availability are considered, as some assumptions in the High availability scenario do not comply with the sustainability criteria defined by the European Commission’s revised Renewable Energy Directive

2018/2001/EU (RED II) (“Member States shall grant no support for the use of saw logs, veneer logs, stumps and roots to produce energy”)¹¹. Additionally, this analysis only considers primary forestry residues (ENSPRESO dataset codes MINBIOFSR1 and MINBIOFSR1a) and excludes secondary residues e.g., from the wood processing industry, thus complying with the assumptions made in the technoeconomic and environmental analysis (sections 2.3 and 2.5).

The biomass potentials for energy purposes, as contained in the ENSPRESO dataset, are mainly distributed among electricity generation, use for heating, and biofuels production. The biomass distribution between these three applications differs in the literature on the topic. In most studies, the largest part of the biomass for energy purposes is used for heating and typically makes up around 65 to 70 % of the available biomass^{71, 72}. The biomass used for electricity generation makes up around 15 %^{71, 72}. Consequently, around 15 to 20 % of the biomass potential is used for the production of biofuels, which are again distributed among the different transportation sectors, with aviation and shipping being the main recipients after 2040. To our knowledge, there are currently no studies that disaggregate the different sources of biomass, such as forestry residues, to the different applications. Thus, we assume for this analysis that 33 % of the forest residue biomass potential is used for aviation biofuels.

2.7. Process analysis under local boundary conditions

To evaluate PBtL production costs and GHG emissions under local European boundary conditions, a techno-economic and emission analysis on an NUTS2 level was performed. A region’s economic attractiveness as a PBtL plant site is determined by local biomass prices, labour costs and electricity price. The local emissions are dependent on the location-specific biomass transport radius and the GHG footprint for the electricity production. Here, NUTS2-specific PV, on-shore wind and the national grid are considered as sources for electricity.

2.7.1. Local production cost. National electricity prices are taken from the Eurostat database⁷³ for large scale consumers (>150 GWh) in the first half of the year 2020 excluding VAT and other recoverable taxes and levies. Where no data is available for 2020, prices for past years are used. If no prices are listed in this category, the calculation relies on price data from consumers from 70 GWh to 150 GWh. Labour costs are taken from the Eurostat dataset⁷⁴. The used national values for electricity price and labour cost can be found in the ESI.

To estimate the levelised cost of electricity (LCOE) for renewable energy sources, maintenance and investment cost are considered in Eq. 6. For both PV and onshore wind capital expenditure (CAPEX) are considered as shown in Tab. 5⁶, whereby a lifetime t of 25 years is assumed for both technologies. With the maintenance factor mf annual maintenance costs are estimated as 1.5 % (PV) or 2.5 % (wind) of the investment ⁶. With the capacity factor cf the number of full load hours per year can be accounted for.

$$LCOE \left[\frac{\text{€}}{\text{MWh}} \right] = \frac{\text{CAPEX} \left[\frac{\text{€}}{\text{MW}} \right]}{t \text{ [a]}} + \frac{\text{CAPEX} \left[\frac{\text{€}}{\text{MW}} \right] \cdot mf \left[\frac{\%}{\text{a}} \right]}{cf \cdot 8760 \left[\frac{\text{h}}{\text{a}} \right]} \quad \#(6)$$

The capacity factors cf for all European NUTS2 regions are taken from the ENSPRESO dataset⁷⁰. In this study, the capacity factor

Tab. 5. Investment cost for hydrogen generation units^{6,7}.

CAPEX	M€/MW
Onshore wind	1.53
PV	0.86
AEL	1

for the average top 50 % wind spots is used. For PV, global ground irradiation values are used to determine the cf .

The local biomass cost is calculated as the sum of feedstock and transport costs. The local biomass feedstock price for forest residue is calculated as the average of its subcategories, wood residue, chip and pellets, and landscaping residues, for the medium availability scenario in the ENSPRESO dataset^{69,70}. The biomass transport cost is found as a function of the transport distance to the plant. The local biomass density ρ determines the feedstock sourcing area A , which is required for a 400 MW_{th} biomass input W . The average transport radius r^* follows from Eq. 8. The biomass transport cost is obtained by multiplying local transport cost, as documented in the ESI, with the average transport radius r^* .

$$A = \frac{W}{\rho} \quad \#(7)$$

$$r^* = \sqrt{\frac{A}{2\pi}} \quad \#(8)$$

In cases where the NUTS2 area doesn't supply enough biomass for a 400 MW_{th} plant, i.e. 13 PJ/a, it is assumed that biomass can be imported at the area's own transport and feedstock costs from neighbouring NUTS2 areas. For the calculation of the transport radius no availability limitations, as described in 2.6, are considered.

2.7.2. Local GHG emissions. The carbon intensity for all considered national grid mixes can be found in the ESI¹. PV and wind emissions are calculated based on their local capacity factor. Wind energy is considered to have a footprint of 7.9 g_{CO_{2,eq}}/kWh at 3600 h/a and PV 47 g_{CO_{2,eq}}/kWh at 1200 h/a⁷⁵.

Emissions from biomass transport are scaled by the transport radius. The base case transport radius of 100 km has emissions of 2.3 g_{CO_{2,eq}}/MJ as calculated in the ESI.

Based on emissions and production cost, NUTS2 specific GHG abatement costs are determined. This value represents the premium of producing green SAF instead of using fossil fuels.

For the GHG abatement costs calculation according to Eq. 9, a crude oil price of 75 \$/barrel⁷⁶, i.e., 0.42 €/l, and GHG emissions from fossil fuel $m_{\text{CO}_2,eq,crude\ oil}$ of 94 g_{CO_{2,eq}}/MJ⁷⁷ are assumed.

$$\text{GHG Abatement cost} \left[\frac{\text{€}}{\text{tCO}_2} \right] = \frac{\text{Price}_{\text{PBtL}} - \text{Price}_{\text{crude oil}}}{m_{\text{CO}_2,eq,crude\ oil} - m_{\text{CO}_2,eq,\text{PBtL}}} \quad \#(9)$$

2.7.3. Integration scenarios for fluctuating energy sources. A continuous H₂ supply from the electrolyser is required for a steady-state operation of the PBtL plant. To accomplish this for the fluctuating renewable resources, wind and PV, two idealised scenarios are considered in this study, as displayed in Fig. 2:

- 1. Virtual grid scenario:** The fluctuating energy input is turned into a stationary profile by a virtual grid. As no additional costs are associated with the virtual grid, this can be regarded as an optimistic scenario.
- 2. Hydrogen storage scenario:** The electrolyser is operated flexibly. The resulting fluctuating hydrogen output is then stored in hydrogen tanks or suitable cavern storage with a constant output. To match the hydrogen demand of the process, the electrolyser has to be over-dimensioned entailing additional investment cost. The electrolyser size increases with decreasing capacity factor of the energy source. The additional cost for hydrogen storage is not considered here.

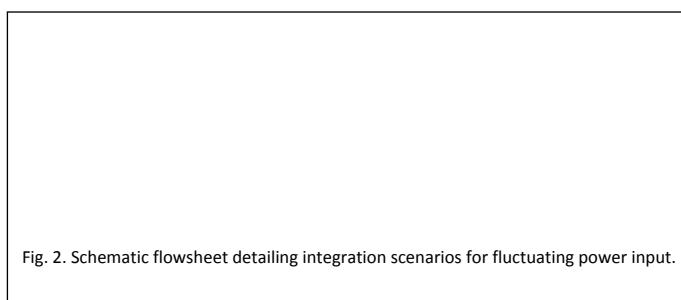


Fig. 2. Schematic flowsheet detailing integration scenarios for fluctuating power input.

2.8. Limitations of the analysis methodology

All presented technical, economic and ecologic assumptions underlie different levels of uncertainty. The uncertainty for any basic process design cost study is typically given within the range of $\pm 30\%$ ⁹. To make the uncertainty in the economic results more transparent, a sensitivity analysis for the most impactful economic parameters in the base case is performed. Similarly, the ecological impact is discussed with a sensitivity analysis. Here, the GWP of PBtL production is discussed as a function of the GWP of the used electrical power.

For the local analysis, a number of assumptions on top of the base case analysis have to be highlighted for their uncertainty. The availability of forest residue for fuel production is assumed to be 33 % NUTS2 regions. These percentages will be determined by political or economic processes in the future and are therefore hard to predict. Additionally, it is assumed that it will be possible to construct PBtL plants in all NUTS2 regions. This neglects the possibility that certain factors, such as lacking social acceptance, might make it impossible to produce fuel in these regions. Also, the availability of all required in process units is assumed. Nevertheless, the availability of enough electrolyzer units might prove to be a bottleneck for the process

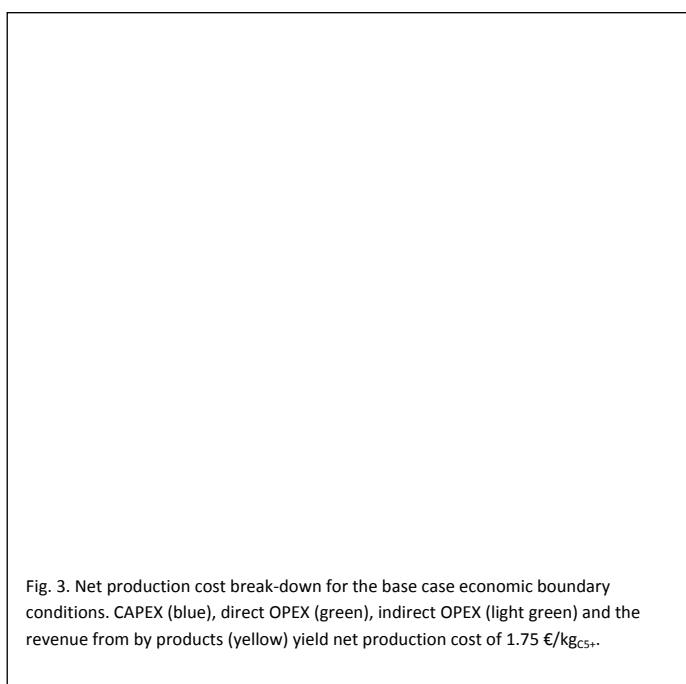
roll-out⁷⁸. Further, the simplified approach for the integration scenarios, as described in section 2.7.3, should only be understood as an approximation of the actual costs for the integration of fluctuating renewable energy sources. A more accurate process design would include a cost-optimised design of the power production system (mix of wind and PV), the electrolyzer and the hydrogen storage system depending on local boundary conditions.

Regarding the LCA, the current study uses the ecoinvent version 3.7.1 and the impact assessment methods as implemented in this version to model and assess the PBtL pathway. At the time of publication however, a newer ecoinvent version with updated datasets and LCIA methods has been made available. Even though this does not affect the foreground modelling, the final results of the analysis using the newest ecoinvent version are expected to be slightly different from the ones presented here due to the updates in the background processes. The updated EF 3.0 methods should also be used in place of the ILCD 2.0 2018 / EF 2.0 methods used in this study.

Finally, another limitation lies in the lack of regional data for the LCA of the PBtL pathway. Should such data become available in the future, it is highly recommended to adapt the analysis to correspond to the regional circumstances of the system under evaluation.

3. Results and Discussion

In this section, an analysis of the base case is presented, including a techno-economic analysis and a life cycle assessment. Based on the results, the impact of important process parameters on the process performance is discussed with a sensitivity analysis. Secondly, the results of the Europe-wide location-specific techno-economic and GHG emission analysis are shown. Their implications for the European SAF production are discussed assuming different integration scenarios for various electrical energy sources.



3.1. Base case evaluation

3.1.1. Technical process evaluation. Mass and energy balances derived from the Aspen Plus[®] model are displayed in Tab. 6. A more detailed version of the balances can be found in the ESI along with the T-H diagram showing the process heat integration. The corresponding process performance indicators can be taken from Tab. 6 as well. Here, the relatively high carbon conversion of 92% is due to full CO₂ and high FT off-gas recycling. Around 45 % of the

Tab. 6. Mass and energy balances for the PBtL process and resulting efficiency values.

Input	
Biomass [MW _{LHV}]	400
Biomass 50 % _{moist.} mass flow [kg _{wet} /s]	47.36
LHV 50 % _{moist.} [MJ/kg]	8.45
Total el. Power [MW _{el}]	943.6
Power input electrolyser [MW _{el}]	890.1
Total power input [MW]	1343.6
Output	
Product [MW _{LHV}]	602.4
Product mass flow [kg _{C5+} /s]	13.72
Carbon content [% _{wt.}]	85
Product LHV [MW _{LHV}]	43.91
Low pressure steam [MW _{LHV}]	179
Medium pressure stream [MW _{LHV}]	57.4
High pressure steam [MW _{LHV}]	95.3
Total power output [MW]	934.2
Process efficiency	
Carbon conversion X_C [%]	92
Biomass conversion X_{biom} [%]	29
Fuel efficiency η_{fuel} [%]	45
Process efficiency $\eta_{process}$ [%]	70

energy input can be converted to fuel and another 25 % to steam.

3.1.2. Production cost estimation. For the base case, location-specific economic boundary conditions typical for Finland are considered⁵ as defined in section 2.4. Overall, net production cost (NPC) of 1.75 €₂₀₂₀/kg are found for the base case. This amounts to 1.32 €₂₀₂₀/l or 39.9 €₂₀₂₀/GJ. Fig. 3 shows the production cost split by the contributing cost fractions. Operational expenditures (OPEX), in green, represent the largest cost share. It is apparent that OPEX are dominated by costs for the electrical power followed by the biomass cost. Similarly, investment costs, depicted in blue, are dominated by the electrolyser cost.

Life Cycle Assessment. The LCA results for the base case following the methodology introduced in section 2.5 are discussed here.

As already mentioned, an economic allocation was applied to account for the revenues of the by-products. The resulting allocation factors are listed in the ESI. Approximately 90% of the resulting environmental impacts are allocated to the FT product.

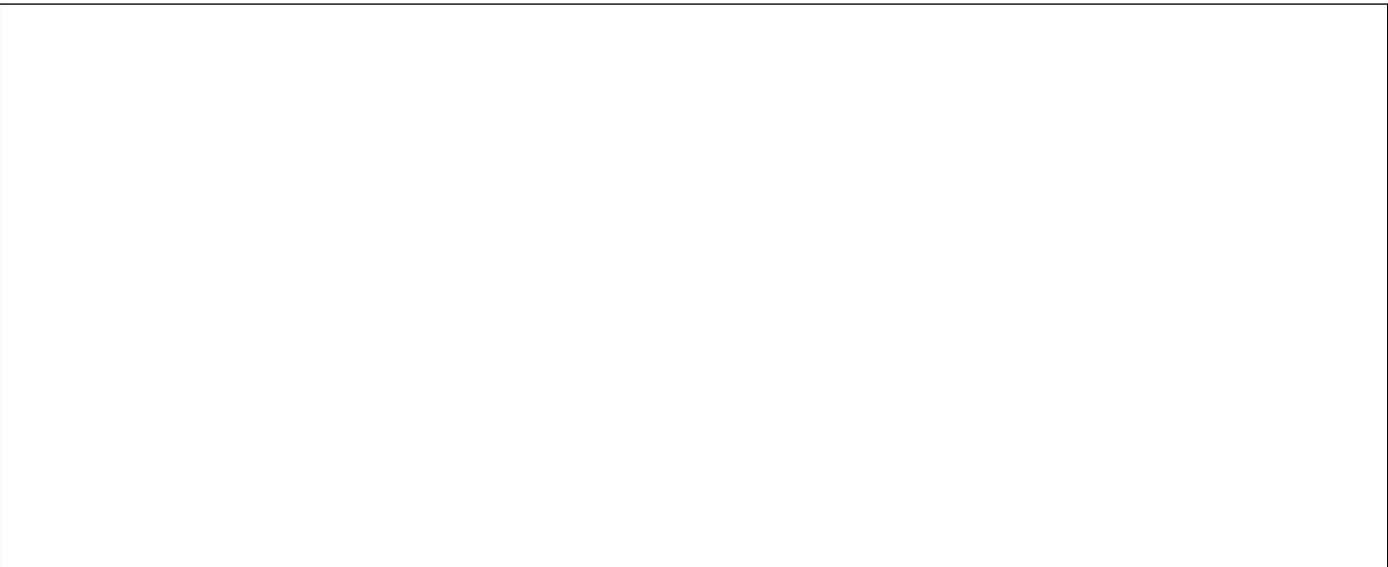


Fig. 5. Relative environmental impacts of the PBtL production processes in different impact categories for the case of electricity from wind turbines. (AP: Acidification; ECF: Energy carriers, fossil; FEP: Eutrophication, aquatic freshwater; FETP: Ecotoxicity (freshwater); GWP: Global Warming Potential; LU: Land use; MEP: Eutrophication, aquatic marine; MM: Minerals and metals; ODP: Ozone depletion; PM: Particulate matter/ Respiratory inorganics; POF: Photochemical ozone formation; TEP: Eutrophication, terrestrial; WS: Water scarcity).

It must be noted that the biogenic carbon that is captured during forest growth was not considered in the life cycle inventories. This has to be considered when modelling the entire life cycle of the fuel. In a simplified model the CO₂ captured by the biomass is emitted again during combustion of the PBtL fuel thus resulting in a net zero CO₂ emission when the

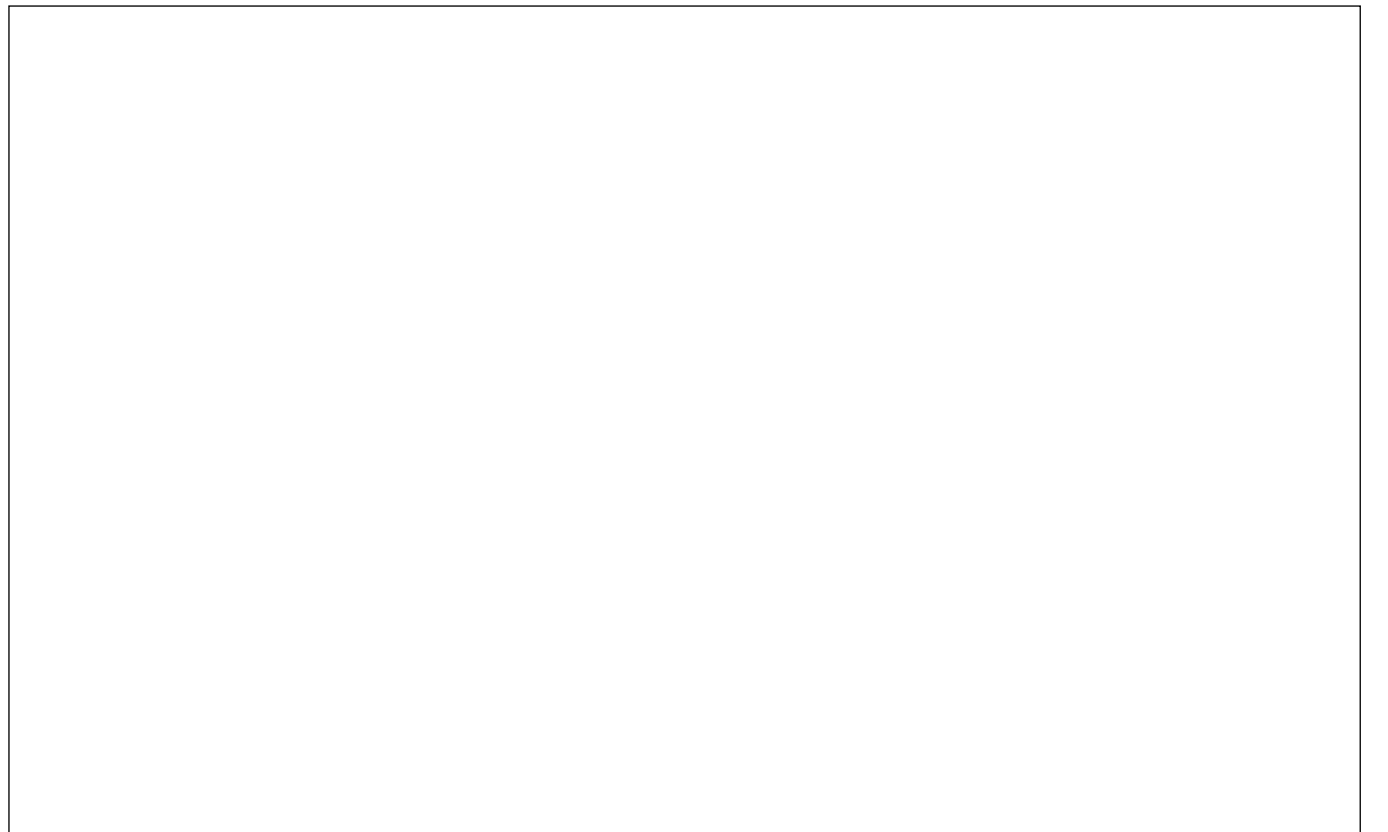


Fig. 4. Absolute environmental impacts from PBtL production using renewable energy from wind turbines or photovoltaic panels compared to the fossil kerosene production. (AP: Acidification; ECF: Energy carriers, fossil; FEP: Eutrophication, aquatic freshwater; FETP: Ecotoxicity (freshwater); GWP: Global Warming Potential; LU: Land use; MEP: Eutrophication, aquatic marine; MM: Minerals and metals; ODP: Ozone depletion; PM: Particulate matter/ Respiratory inorganics; POF: Photochemical ozone formation; TEP: Eutrophication, terrestrial; WS: Water scarcity).

fuel is used. This simplified assumption of biogenic carbon neutrality does not consider carbon stock changes in the forest. For a more accurate estimation of the GHG emission savings, all relevant forest carbon pools need to be considered in the analysis as well as their evolution within relevant time horizons⁷⁹. Moreover, the evaluation in terms of climate change impact of the entire lifecycle of the fuels (including combustion) when used in aviation needs to consider the non-CO₂ effects of inflight emissions in the atmosphere (mostly due to the positive radiative forcing of contrails⁸⁰.) These effects are, however, not discussed here since the scope of the analysis is restricted to the fuel production.

Fig. 5 illustrates the relative contribution analysis of the different steps involved in the PBtL production for the case of electricity from wind turbines used for the production of PBtL. In more detail, a high percentage of the contribution to acidification (AP) stems from the emissions during PBtL production (mostly ammonia from the Selexol scrubbing step). Around half of the contribution to the use of fossil energy carriers (ECF) originates from the fossil resources needed for the construction of wind turbines for electricity. The majority of the remaining impact in this category is caused by the fossil fuels used during transportation and provision of the biomass. In the category of freshwater eutrophication (FEP), the main burdens can be attributed to the treatment of wood ash, which is for example used in landfarming (modelled as part of the emissions of the PBtL process). The construction of wind turbines (mainly steel production) and the wastewater emissions during the production of oils used in the forestry machines for biomass provision also contribute to this category. In the category of freshwater ecotoxicity (FETP), the main impacts can be attributed to the treatment of wood ash and the burdens from steel needed to manufacture wind turbines (contained in the category electricity). The contributions in the category of Global Warming Potential (GWP) are distributed mainly among the burdens from the construction of wind turbines, the emissions of the PBtL production process itself (predominantly off-gas emissions), the biomass transport, and the biomass provision. Here, the biogenic as well as the fossil carbon emissions are included in the model. In the category of land use (LU), the main contribution stems from the biomass provision. In terms of marine eutrophication (MEP), the impacts result from the ammonia emitted during the PBtL production process itself, as well as the nitrogen oxides and ammonia emitted both during wind turbine construction and to a smaller extent from the biomass provision and transportation. In the category of minerals and metals (MM), the main contribution originates from the copper needed for electricity generation and transmission. Smaller contributions stem from the cobalt catalyst and the PBtL plant construction. The ozone depletion (ODP) is a result of gases emitted during the production of petroleum, which is mainly used for biomass transport and biomass provision (forestry equipment) in the PBtL process chain as well as in the construction of wind turbines. The impact on human health from particulate matter (PM) mainly stems from the ammonia emitted during PBtL production and particulates emitted in processes involved in the construction

of wind turbines or during the biomass transport. The photochemical ozone formation (POF) can be attributed mainly to the nitrogen oxides and non-methane volatile organic compounds (NMVOCs) emitted in processes involved in the construction of wind turbines or during transport of biomass and biomass provision (e.g., power sawing). The main contribution to terrestrial eutrophication (TEP) can be attributed to the emission of ammonia during PBtL production. Finally, the impact on water scarcity mainly stems from the water dissipated in the processes involved in the construction of wind turbines.

Fig. 6. Effect of the electricity GWP on fuel GWP (left axis) and GHG abatement cost (right axis). National grid GWP in Sweden ($9 \text{ g}_{\text{CO}_2, \text{eq}}/\text{kWh}_{\text{el}}$), France ($51 \text{ g}_{\text{CO}_2, \text{eq}}/\text{kWh}_{\text{el}}$), EU-27 ($231 \text{ g}_{\text{CO}_2, \text{eq}}/\text{kWh}_{\text{el}}$) and Germany ($311 \text{ g}_{\text{CO}_2, \text{eq}}/\text{kWh}_{\text{el}}$)¹ are shown alongside the calculated GWP range for PV (orange: $7\text{--}24 \text{ g}_{\text{CO}_2, \text{eq}}/\text{kWh}_{\text{el}}$) and on-shore wind (blue: $29\text{--}77 \text{ g}_{\text{CO}_2, \text{eq}}/\text{kWh}_{\text{el}}$)⁶. As reference the GWP of fossil fuel ($94 \text{ g}_{\text{CO}_2, \text{eq}}/\text{MJ}$) and the GWP limit for SAF as defined in the RED II directive ($32.9 \text{ g}_{\text{CO}_2, \text{eq}}/\text{MJ}$)¹¹ are also shown. Base case electricity and biomass price are used to calculate the GHG abatement cost.

For a better notion of the magnitude of the environmental impacts in absolute terms, Fig. 4 depicts the results of the production of PBtL according to the base case with electricity from wind turbines or photovoltaic panels and compares these two cases to the production of kerosene from fossil fuels. The latter was taken from the ecoinvent database (“kerosene production, petroleum refinery operation in Europe without Switzerland”). It should be noted that all impacts of the kerosene burning process are not included, which are significant e.g. for the GWP category. Due to the higher burdens associated with the production of photovoltaic panels compared to wind turbines, the PBtL from solar energy performs worse than the PBtL from wind energy in all selected impact categories. In many categories the PBtL fuel has a significantly higher impact compared to fossil kerosene, e.g., in the resource category minerals and metals as well as water scarcity, because of the high amounts of metals and water needed for renewable electricity production, respectively. The impact on land use is also significantly higher due to the provision of biomass.

A better management of the gaseous and wastewater emissions of the PBtL plant should result in a reduction of the impacts of the PBtL process, especially in the categories AP, TEP, PM, GWP, and MEP. A further increase in efficiency of renewable energy sources in combination with the use of recycled materials in the production of wind turbines and photovoltaic panels may further reduce the impacts in the categories where electricity has a high contribution. Finally, should more sustainable fuels

be used in the transport and provision of biomass in the future, a reduction of these impacts in the relevant categories could be achieved.

3.1.3. Sensitivity analysis

The presented cost estimates and LCA results are based on a

Fig. 7. Parameter variation showing the effect of electricity and biomass prices on the PBtL production cost.

number of assumptions that may vary depending on location and time of analysis. To account for this, biomass and electricity

price, as the two most important OPEX factors (cf. Fig. 3), are subjected to a sensitivity analysis. A realistic range for forest residue biomass can be stated as 20.3 to 102.5 €/t³⁹. The ENSPRESO dataset, which was used to estimate local production costs in section 3.2.2, reports biomass prices in the range of 16.6 to 64.8 €/t_{50%moist.}⁶⁹ for Europe. Similarly, grid electricity prices can range from 30.8 €/MWh_{el} in Norway to 136.1 €/MWh_{el} in the UK⁷³.

Fig. 8. Biomass potential for ENSPRESO MED scenario assuming 33 % availability for SAF production.

Fig. 7 depicts the impact of both commodity prices on the PBTL process's production costs. The outsized impact of the electricity price can be seen here: a 20% reduction in electricity price reduces production cost by 0.21 €/kg_{C5+}. A 20% decrease in the price of biomass, on the other hand, only results in a 0.03 €/kg_{C5+} reduction in production cost.

Tab. 7. Biomass potential from primary forestry residues for energy uses in Europe as calculated in this analysis and compared to literature (harmonised to primary residues expressed in EJ/a).

Source	Potential	Year	Comment
This study, LOW scenario	1.12 EJ/a	2030	
This study, MED scenario	2.24 EJ/a	2030	
Searle and Malins, 2013 ²	0.76 EJ/a	2030	Only EU (derived from 40 Mt with 19 GJ/t)
BRE, 2015 ⁸	2.2 EJ/a	2030	EU, Technical-energy (TE) potential
BRE, 2015 ⁸	0.44 EJ/a	2030	EU, Sustainable (S) potential
Searle and Malins, 2015 ¹⁵	0.41 EJ/a	2030	Forestry residues w/o amount retained for soil quality
Imperial College London Consultants, 2021 ¹⁹	0.71 EJ/a	2030	Primary forestry residues, Low scenario
Imperial College London Consultants, 2021 ¹⁹	1.13 EJ/a	2030	Primary forestry residues, High scenario
This study, LOW scenario	0.56 EJ/a	2050	
This study, MED scenario	2.24 EJ/a	2050	
Smeets et al., 2007 ²⁵	1 EJ/a	2050	Wood harvest residues, West & East Europe
Haberl et al., 2010 ²⁸	2 EJ/a	2050	Mean value only considering primary residues
Lauri et al., 2014 ²⁹	ca. 1.5 EJ/a	2050	EU27 (derived from Fig. 6 with 7.2 GJ/m ³)
Imperial College London Consultants, 2021 ¹⁹	1.13 EJ/a	2030	Primary forestry residues, High scenario

As previously shown in Fig. 5, the contribution to the FT fuel's GWP of the electricity production is substantial, even when on-shore wind production with a footprint of 11.3 g_{CO2}/kWh_{el} is considered. The full range of the electricity GWP impact on the

fuel GWP is shown in Fig. 6. Here, the fuel GWP is represented by the blue line referring to the left y-axis. The fuel's GWP rises linearly with the carbon intensity of the electricity production. With an electricity GWP of 214 g_{CO2,eq}/kWh_{el}, FT fuel has the same GWP as fossil fuel (94g_{CO2,eq}/MJ)¹¹. Consequently, PBTL fuel produced with the German or European average grid mix of the year 2020 has a stronger climate effect than fossil fuel combustion. To qualify as sustainable fuel according to the RED II directive¹¹ (< 32.9 g_{CO2,eq}/MJ), the electricity GWP must be lower than 63 g_{CO2,eq}/kWh_{el} under the assumed boundary conditions. As a result, only countries with a less carbon-intensive electricity grid mix, such as France or Sweden¹, should be considered as production sites for grid-connected PBTL production.

In Fig. 6 the GWP intensity range found for PV and wind power in all NUTS2 regions is displayed. PBTL fuel produced with wind power can be counted as SAF according to the RED II without any exceptions. Yet, PV production in northern European NUTS2 regions can exceed this limit.

The GHG abatement cost, as defined in Eq. 9, is depicted in Fig. 6 with the green line referring to the right y-axis. The abatement cost increases exponentially with the electricity's GWP and approaches infinity when the FT fuel has the same GWP as fossil fuel at 214 g_{CO2,eq}/kWh_{el}. On the lower end, the abatement costs approach 339 €/t_{CO2,eq} when assuming the base case electricity and biomass price.

3.2. European SAF production potential

A NUTS2-specific analysis was performed to estimate the potential amount and production cost of SAF that can be produced from European forest residue. Section 3.2.1 provides an overview of Europe's forestry residue potential. Based on that, the region-specific

production costs for grid-connected PBTL operation are discussed. Subsequently, results for renewable fluctuating energy sources are presented, whereby it is distinguished between the two integration scenarios, virtual grid and hydrogen storage, described in section

2.7.3. Finally, the fuel's GWP footprint and GHG abatement cost for every NUTS2 region is shown.

3.2.1. European biomass potential from forestry residues. The local distribution of forestry residue for the ENSPRESO MED scenario can be taken from Fig. 8. It is apparent that especially northern European and Baltic NUTS2 regions have a large forest residue potential.

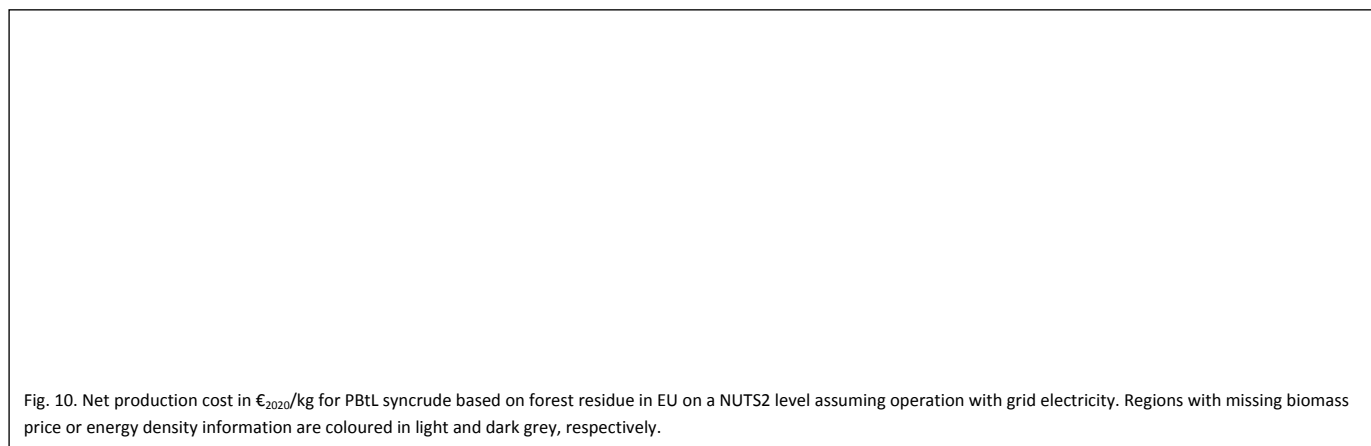


Fig. 10. Net production cost in $\text{€}_{2020}/\text{kg}$ for PBtL syncrude based on forest residue in EU on a NUTS2 level assuming operation with grid electricity. Regions with missing biomass price or energy density information are coloured in light and dark grey, respectively.

The resulting total biomass potential from primary forestry residues available for energy uses as extracted from the ENSPRESO database can be seen in Tab. 6. It can be seen that in the Medium bioenergy availability scenario (MED) the potential is assumed as almost constant between 2030 and 2050. In the Low availability scenario (LOW) on the other hand, the potential is expected to decrease in the future. A comparison to other studies is also shown in Tab. 6. The highest predicted biomass potentials in other studies fall within the same range as the ones from the ENSPRESO dataset. Some of the other studies forecast lower potentials, which can be explained with stricter sustainability limitations assumed in their scenarios. It must also be noted that some discrepancies in the data from the various studies may stem from different definitions of primary forestry residues (e.g., wood harvest residues) or from slightly different geographical scopes (e.g., EU vs. Europe). Due to the unavailability of more detailed data, it was however not possible to eliminate these inconsistencies between the different datasets. The electricity demand for Europe wide PBtL production would amount to around 5.3 EJ/a in 2030 and 2050 assuming full utilization of the forest residue in the the MED scenario. According to the ENSPRESO database, the PV (40 EJ/a) and wind (30 EJ/a) potential in Europe indicate that forest residue is the limiting resource for the PBtL process⁷⁰. Other technical constraints could also prove to be the bottleneck for a European PBtL roll-out. The total electrolyser capacity, for instance, is aimed to be ramped up to only 1.2 EJ/a hydrogen output by 2030⁸¹. Nevertheless, in this study only forest residue is treated as the limiting factor.

3.2.2. Region-specific production cost. Grid-connected local NPC for Europe on a NUTS2 level can be taken from Fig. 10. The production costs are in a range from 1.5–4 $\text{€}_{2020}/\text{kg}$ of Fischer-Tropsch product. The best conditions for the PBtL plant can be found in Northern European countries and parts of Belgium and Bulgaria. As shown in section 3.1.3, the electricity price plays a

dominant role for the NPC. Accordingly, the lowest NPC can be found in Norway, 1.47 $\text{€}_{2020}/\text{kg}_{\text{C5+}}$, having the most inexpensive grid power at 30.8 $\text{€}/\text{MWh}_{\text{el}}$ ⁷³.

Fig. 11 and Fig. 9 show local production costs for PBtL plants operated with on-shore wind and PV energy. In both figures the results for the hydrogen storage scenario are displayed (c.f. section 2.7.3). In this integration scenario for renewable

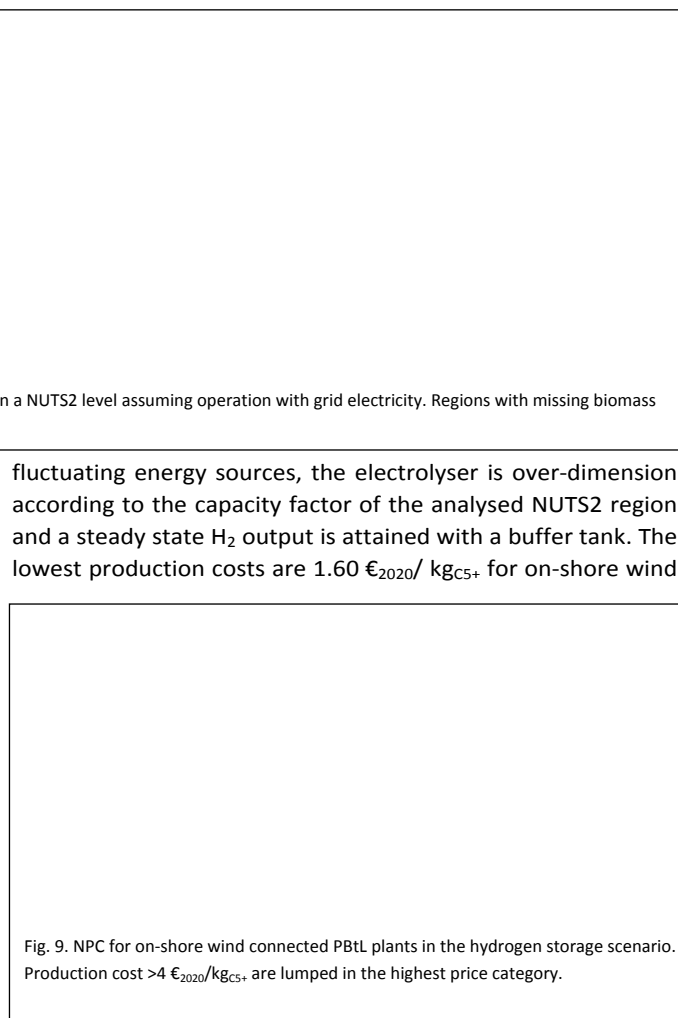


Fig. 9. NPC for on-shore wind connected PBtL plants in the hydrogen storage scenario. Production cost $>4 \text{€}_{2020}/\text{kg}_{\text{C5+}}$ are lumped in the highest price category.

energy and 2.50 $\text{€}_{2020}/\text{kg}_{\text{C5+}}$ for PV.

In the optimistic virtual grid scenario, the fluctuating energy input is assumed to be converted to a steady power input for the electrolyzer without any additional cost. In this scenario, production costs as low as 1.23 $\text{€}_{2020}/\text{kg}_{\text{C5+}}$ for wind and 1.22 $\text{€}_{2020}/\text{kg}_{\text{C5+}}$ for PV were found. The price discrepancy between the scenarios is due to the additional cost for the over-dimensioned electrolyser.

For both scenarios, the production costs are highly dependent on the local capacity factor. Accordingly, the lowest production cost for wind energy can be found in coastal regions in Northern

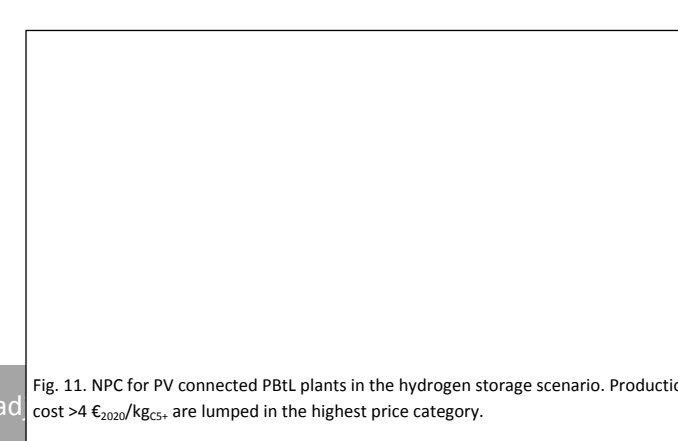


Fig. 11. NPC for PV connected PBtL plants in the hydrogen storage scenario. Production cost $>4 \text{€}_{2020}/\text{kg}_{\text{C5+}}$ are lumped in the highest price category.

and Western Europe. PV has the strongest prospect in Southern Europe.

3.2.3. Local GHG abatement cost. For many countries in Europe abating GHG emissions with PBtL production is impossible due to the emission intensity of their national grid mix. In all dark red NUTS2 regions in Fig. 13, the production of PBtL fuel leads to higher emissions than fossil fuel. Even countries with promising NPC, such as Bulgaria with under 2 €₂₀₂₀/kg_{C5+}, produce with a higher GWP than fossil fuel. Only countries with low-GHG and in-expensive electricity

3.2.4. Aggregated PBtL SAF production potential. The combined potential SAF production volume over all NUTS2 regions with a GWP under the RED II limit of 32.9 g_{CO_{2,eq}}/MJ_{fuel} is shown in Fig. 12. Here, it is assumed that 33 % of forest residues can be used for SAF production. In addition, the aggregated fuel potential is sorted by production cost categories. All PBtL production scenarios can be compared to the Biomass to Liquid (BtL) production route, for which a biomass conversion of 19.9 % is assumed.

Fig. 12. European SAF production potential with a GWP under 32.9 g_{CO_{2,eq}}/MJ_{fuel}. The potentials are calculated with the assumption that 33% of all forest residue can be used for fuel production. The different power integration scenarios grid, hydrogen storage (H2) and virtual grid (VG) are compared with a biomass to liquid (BtL) process, which has a biomass conversion of 19.9 %. The ReFuel EU blending targets of 32% in 2040 and 63% in 2050 are applied to the 2030 European aviation fuel demand of 62.8 Mt/a.

reach fairly low GHG abatement cost. The lowest abatement cost is found in Norway with 288 €₂₀₂₀/t_{CO_{2,eq}}. As of the year 2020, only PBtL fuel produced in France, Norway, Sweden and Lithuania has a GWP footprint lower than the 32.9 g_{CO_{2,eq}}/MJ necessary for SAF production according to the RED II directive¹¹. This might change in the future as many countries are in the process of decarbonizing their national grid mix.

The high GWP grid mix in many countries makes PBtL fuel production under the RED II directive currently impossible as shown in section 3.2.3. The BtL process, which requires only a marginal electrical power input, is not reliant upon low-GWP electricity. Thus, grid connected PBtL has a lower SAF potential than BtL.

With the renewable energy sources wind and PV, a fuel output

Fig. 13. GHG abatement cost map for a grid connected PBtL process. NUTS2 regions with no abatement are marked in dark red.

The PBtL production in the hydrogen storage scenario with on-shore wind turbines yields an abatement cost as low as 337 €₂₀₂₀/t_{CO_{2,eq}} and 662 €₂₀₂₀/t_{CO_{2,eq}} for PV production. In the virtual grid scenarios, the lowest abatement cost is found at 208 €₂₀₂₀/t_{CO_{2,eq}} for wind and 237 €₂₀₂₀/t_{CO_{2,eq}} for PV. Abatement cost maps for all discussed cases can be found in the ESI. No NUTS2 region has higher GWP emissions than fossil fuel. But, for a few Northern European regions PV powered production leads to a higher footprint than defined in the RED II directive.

of around 25 Mt/a can be reached. The PV output is slightly lower as some Northern European NUTS2 regions exceed the REDII limit due to their low capacity factor. However, the production volume suffices for the 2040 ReFuel EU goal of 20.1 Mt/a²², i.e., 32 % of the estimated 2030 European fuel demand of 62.8 Mt/a²¹. For the 2050 goal of 63 % either a higher share of forest residue for fuel production or the use of additional renewable feedstocks, such as agricultural residues or municipal waste, are required.

The renewable energy integration scenario is crucial for the production cost. While the bulk of the product can be produced

for under $2 \text{ €}_{2020}/\text{kg}_{\text{C}_{5+}}$ with the virtual grid (VG), the hydrogen storage scenario (H2) results in production costs over $2 \text{ €}_{2020}/\text{kg}_{\text{C}_{5+}}$.

4. Conclusions

In this study, sustainable aviation fuel (SAF) production via the Power Biomass to Liquid (PBtL) route was evaluated in terms of an immediate European deployment. A techno-economic analysis and life cycle assessment (LCA) of a $900 \text{ MW}_{\text{el}}$ and $400 \text{ MW}_{\text{th}}$ PBtL process producing 0.4 Mt/a FT fuel have been conducted based on an Aspen Plus[®] flowsheet simulation. The national grid, on-shore wind and PV have been considered as power sources. To account for region-specific utility costs, forest residue potentials and the GWP of regionally available electricity in Europe, a techno-economic and environmental analysis methodology has been applied in around 300 European NUTS2 regions. The results of this study show how much and at what cost SAF can be produced in Europe via the PBtL route.

Green and inexpensive electricity is essential for economic and sustainable fuel production via the PBtL process. Only a few national grids currently have a GWP low enough to achieve a 65% GWP reduction for SAF compared to fossil fuel. Consequently, the PBtL process should currently be regarded as a sweet spot solution for countries like Norway, Sweden or France. Since many countries are in the process of reducing the GWP of their power production¹, the PBtL process could become more broadly applicable in the future. In the meantime, an off-grid system could be considered for production sites with high renewable power generation potential. Ireland, for instance, would serve as an excellent PBtL production site due to its high wind potential. Here, the integration of the fluctuating power supply is crucial for the process economics, as an over-dimensioned electrolyser can have a significant impact on the SAF production costs.

The availability of biomass residues has been identified as another limiting factor, besides green and inexpensive electricity. Around 25 Mt/a of SAF can be produced in Europe, assuming that 33% of all forestry residue available for energy purposes can be used for fuel production. This would cover the 32% blending rate mandated in the ReFuel EU directive²² for the year 2040. To reach the entire European aviation fuel demand of 62.8 Mt/a , either a larger share of forest residue has to be used for fuel production or other feedstock types, such as agricultural residue or municipal solid waste. Yet, the demand for all biomass residues is bound to increase as they also serve as feedstock for low-carbon heat and power production. In situations with a high demand for biomass residues, the advantage of the PBtL process' near full carbon conversion should be considered when allocating these limited resources.

The following points should be considered in future work on this topic:

- The process configuration is fixed with the base case. The optimal plant configuration at each individual site might vary with the regional boundary conditions. For

example, a slight reduction of the CO_2 recycling rate when producing with Finish grid electricity would lower the fuel's GWP. With this slight alteration, Finnish PBtL fuel could be produced according the RED II directive ($< 32.9 \text{ g}_{\text{CO}_2,\text{eq}}/\text{MJ}_{\text{fuel}}$).

- The FT product fraction C_{5+} is treated as SAF in this study. However, additional refining steps are omitted. These steps add further costs to the product and part of the product will not be converted into jet fuel. Taking this into account would improve the accuracy of the cost and fuel volume predictions made here.
- The simulated process relies on a $900 \text{ MW}_{\text{el}}$ AEL. However, the currently largest installed AEL system has a capacity of 10 MW^{82} . Upscaling issues for this technology should be monitored. The development of other technologies, such as SOEC and PEMEL, should also be considered for a future choice of electrolyser.
- No carbon tax for fossil aviation fuel is considered in the calculation of the NPC and GHG abatement cost values of the FT product. The competitiveness of SAF, however, is expected to increase in the future with measures such as the fossil jet fuel tax planned in the EU with the "Fit for 55" legislative package⁸³.
- The assumption that 33% of all forestry residue available for energy purposes can be used for the production of aviation fuel can be considered optimistic. Depending on the demand for other transport and energy applications, this percentage could be significantly lower.
- Only primary forestry residues were considered as biomass feedstock for the derivation of aviation fuel potentials in this study. If other biomass sources were considered as well, these potentials could be significantly higher. Particularly agricultural residues have a high potential and can be similarly sustainable to forestry residues⁸⁴. However, a redesign of the PBtL process, especially the gasification and gas cleaning steps, would be required for these feedstocks.
- Regarding the sustainability of the forestry residues used for fuel production, local forestry management practices need to be assessed carefully in order to ensure that the use of this type of biomass does indeed lead to a significantly lower overall climate impact. Aspects such as land-use change, carbon debt and its payback time have to be considered for each region.

Author Contributions

Conceptualisation, F.H., V.P., R.-U. D., U.B.; Data curation, F.H., V.P.; Formal analysis, F.H., V.P.; Funding acquisition, R.-U. D., U.B.; Investigation, F.H., V.P.; Methodology, F.H., V.P.; Project administration, F.H.; Resources, R.-U. D., U.B.; Software, F.H., V.P.;

Supervision, R.-U. D., U.B.; Validation, F.H., V.P.; Visualisation, F.H., V.P.; Writing – original draft, F.H., V.P.; Writing – review & editing, F.H., V.P., R.-U. D., U.B.

Conflicts of interest

There are no conflicts to declare.

Acknowledgements

The authors would like to gratefully acknowledge the constructive feedback and funding provided by Airbus SE.

References

- European Environmental Agency, Greenhouse gas emission intensity of electricity generation by country https://www.eea.europa.eu/data-and-maps/daviz/co2-emission-intensity-9/#tab-googlechartid_googlechartid_googlechartid_chart_1111, (accessed 31. January, 2022).
- S. Searle and C. Malins, *International Council on Clean Transportation: Washington, DC, USA*, 2013.
- M. Hillestad, M. Ostadi, G. A. Serrano, E. Rytter, B. Austbø, J. Pharoah and O. S. Burheim, *Fuel*, 2018, **234**, 1431-1451.
- F. Habermeyer, E. Kurkela, S. Maier and R.-U. Dietrich, *Frontiers in Energy Research*, 2021, **9**, 684.
- I. Hannula, *Energy*, 2016, **104**, 199-212.
- Agora Verkehrswende, Agora Energiewende and Frontier Economics, *The future cost of electricity-based synthetic fuels*, 2018.
- O. Schmidt, A. Gambhir, I. Staffell, A. Hawkes, J. Nelson and S. Few, *International Journal of Hydrogen Energy*, 2017, **42**, 30470-30492.
- N. Jones, K. Johnson and E. Sutti, *Building Research Establishment Ltd: Liverpool, UK*, 2015, **23**.
- F. G. Albrecht, D. H. König, N. Baucks and R.-U. Dietrich, *Fuel*, 2017, **194**, 511-526.
- European Commission, Revision of the EU ETS Directive concerning aviation, https://climate.ec.europa.eu/eu-action/transport-emissions/reducing-emissions-aviation_en, (accessed 8. February, 2023).
- E. Commission, Renewable Energy – Recast to 2030 (RED II), https://joint-research-centre.ec.europa.eu/welcome-jec-website/reference-regulatory-framework/renewable-energy-recast-2030-red-ii_en, (accessed 24. March, 2022).
- S. A. Isaacs, M. D. Staples, F. Allroggen, D. S. Mallapragada, C. P. Falter and S. R. Barrett, *Environmental Science & Technology*, 2021, **55**, 8247-8257.
- ICAO, ICAO welcomes new net-zero 2050 air industry commitment <https://www.icao.int/Newsroom/Pages/ICAO-welcomes-new-netzero-2050-air-industry-commitment.aspx>, (accessed 10. February, 2023).
- F. G. Albrecht and R.-U. Dietrich, Copenhagen, Denmark, 2018.
- S. Searle and C. Malins, *Gcb Bioenergy*, 2015, **7**, 328-336.
- Q. Bernical, X. Joulia, I. Noirot-Le Borgne, P. Floquet, P. Baurens and G. Boissonnet, *Industrial & Engineering Chemistry Research*, 2013, **52**, 7189-7195.
- K. Dahal, S. Brynolf, C. Xisto, J. Hansson, M. Grahn, T. Grönstedt and M. Lehtveer, *Renewable and Sustainable Energy Reviews*, 2021, **151**.
- C. N. Hamelinck and A. P. Faaij, *Journal of Power Sources*, 2002, **111**, 1-22.
- C. Panoutsou and K. Maniatis, *Sustainable biomass availability in the EU, to 2050*, Concawe, 2021.
- R. M. Swanson, A. Platon, J. A. Satrio and R. C. Brown, *Fuel*, 2010, **89**, S11-S19.
- J. O'malley, N. Pavlenko and S. Searle, *Estimating sustainable aviation fuel feedstock availability to meet growing European Union demand*, International Council on Clean Transportation, 2021.
- European Commission, Proposal for a REGULATION OF THE EUROPEAN PARLIAMENT AND OF THE COUNCIL on ensuring a level playing field for sustainable air transport, https://ec.europa.eu/info/sites/default/files/refueeu_aviation_sustainable_aviation_fuels.pdf, (accessed 17. January 2023).
- M. Prussi, A. O'Connell and L. Lonza, *Biomass and Bioenergy*, 2019, **130**.
- F. Gerard, M. Gorner, P. Lemoine, J. Moerenhout, V. De Haas and P. Cazzola, *Assessment of the potential of sustainable fuels in transport in the context of the Ukraine/Russia crisis*, 2022.
- E. M. Smeets, A. P. Faaij, I. M. Lewandowski and W. C. Turkenburg, *Progress in Energy combustion science*, 2007, **33**, 56-106.
- M. S. Peters, K. D. Timmerhaus and R. E. West, *Plant design and economics for chemical engineers*, McGraw-Hill New York, 2003.
- Eurostat, Preise Gas für Nichthaushaltskunde, ab 2007 - halbjährliche Daten, https://ec.europa.eu/eurostat/databrowser/view/nrg_pc_203/default/table?lang=de, (accessed 30. November, 2022).
- H. Haberl, T. Beringer, S. C. Bhattacharya, K.-H. Erb and M. Hoogwijk, *Current Opinion in Environmental Sustainability*, 2010, **2**, 394-403.
- P. Lauri, P. Havlík, G. Kindermann, N. Forsell, H. Böttcher and M. Obersteiner, *Energy policy*, 2014, **66**, 19-31.
- L. Zhang, T. L. Butler and B. Yang, *Green Energy to Sustainability: Strategies for Global Industries*, 2020, 85-110.
- M. F. Shahriar and A. Khanal, *Fuel*, 2022, **325**.
- E. Rytter and A. Holmen, *Catalysts*, 2015, **5**, 478-499.
- Bechtel, *Aspen Process Flowsheet Simulation Model of a Battelle Biomass-Based Gasification, Fischer-Tropsch Liquefaction and Combined-Cycle Power Plant*, US Department of Energy (DOE) Pittsburgh, Pennsylvania, 1998.
- A. Buttler and H. Spliethoff, *Renewable and Sustainable Energy Reviews*, 2018, **82**, 2440-2454.
- S. De Jong, K. Antonissen, R. Hoefnagels, L. Lonza, M. Wang, A. Faaij and M. Junginger, *Biotechnol Biofuels*, 2017, **10**, 64.
- S. E. Tanzer, J. Posada, S. Geraedts and A. Ramírez, *Journal of Cleaner Production*, 2019, **239**.

37. C. van der Giesen, R. Kleijn and G. J. Kramer, *Environ Sci Technol*, 2014, **48**, 7111-7121.
38. C. M. Liu, N. K. Sandhu, S. T. McCoy and J. A. Bergerson, *Sustainable Energy & Fuels*, 2020, **4**, 3129-3142.
39. G. Haarlemmer, G. Boissonnet, E. Peduzzi and P.-A. Setier, *Energy*, 2014, **66**, 667-676.
40. C. Malins, S. Searle, A. Baral, D. Turley and L. Hopwood, *Wasted: Europe's untapped resource: an assessment of advanced biofuels from wastes and residues*, International Council on Clean Transportation, 2014.
41. E. Kurkela, M. Kurkela and I. Hiltunen, *Biomass Conversion and Biorefinery*, 2021, DOI: <https://doi.org/10.1007/s13399-021-01554-2>, 1-22.
42. V. S. Sikarwar, M. Zhao, P. S. Fennell, N. Shah and E. J. Anthony, *Progress in Energy and Combustion Science*, 2017, **61**, 189-248.
43. P. Basu, *Biomass gasification, pyrolysis and torrefaction: practical design and theory*, Academic press, 2018.
44. G. Wang, J. Zhang, J. Shao, Z. Liu, H. Wang, X. Li, P. Zhang, W. Geng and G. Zhang, *Energy*, 2016, **114**, 143-154.
45. I. Hannula, *Biomass and Bioenergy*, 2015, **74**, 26-46.
46. A. Padurean, C.-C. Cormos and P.-S. Agachi, *International Journal of Greenhouse Gas Control*, 2012, **7**, 1-11.
47. S. LeViness, San Antonio, Texas, 2013.
48. E. Rytter and A. Holmen, *ACS Catalysis*, 2017, **7**, 5321-5328.
49. C. Schnuelle, T. Wassermann, D. Fuhrlaender and E. Zondervan, *International Journal of Hydrogen Energy*, 2020, **45**, 29938-29952.
50. C. Minke, M. Suermann, B. Bensmann and R. Hanke-Rauschenbach, *International Journal of Hydrogen Energy*, 2021, **46**, 23581-23590.
51. E. Kurkela, M. Kurkela, C. Frilund, I. Hiltunen, B. Rollins and A. Steele, *Johnson Matthey Technology Review*, 2021, **65**, 333-345.
52. S. Müller, P. Groß, R. Rauch, R. Zweiler, C. Aichernig, M. Fuchs and H. Hofbauer, *Biomass Conversion Biorefinery*, 2018, **8**, 275-282.
53. Aspen Technology Inc., *Aspen Physical Property System - Physical Property Methods*, 2013.
54. B. Todici, T. Bhatelia, G. F. Froment, W. Ma, G. Jacobs, B. H. Davis and D. B. Bukur, *Industrial Engineering Chemistry Research*, 2013, **52**, 669-679.
55. S. Maier, S. Tuomi, J. Kihlman, E. Kurkela and R.-U. Dietrich, *Energy Conversion and Management*, 2021, **247**.
56. F. Mantei, R. E. Ali, C. Baensch, S. Voelker, P. Haltenort, J. Burger, R.-U. Dietrich, N. v. d. Assen, A. Schaadt, J. Sauer and O. Salem, *Sustainable Energy & Fuels*, 2022, **6**, 528-549.
57. M. Shoaib Ahmed Khan, N. Grioui, K. Halouani and R. Benelmir, *Energy Conversion and Management: X*, 2022, **13**.
58. W.-C. Wang, Y.-C. Liu and R. A. A. Nugroho, *Energy*, 2022, **239**.
59. International Monetary Fund, International Financial Statistics, <https://data.worldbank.org/indicator/PA.NUS.FCRF?locations=XC>, (accessed 12. April, 2022).
60. K. Andersson, S. Brynolf, H. Landquist and E. Svensson, *Shipping and the Environment: Improving Environmental Performance in Marine Transportation*, 2016, 265-293.
61. DIN Deutsches Institut für Normung e.V., 2006.
62. C. Mutel, *Journal of Open Source Software*, 2017, **2**, 236.
63. G. Wernet, C. Bauer, B. Steubing, J. Reinhard, E. Moreno-Ruiz and B. Weidema, *The International Journal of Life Cycle Assessment*, 2016, **21**, 1218-1230.
64. DLR, *Techno economic assessment and LCA report comparing 2-3 process configurations*, 2021.
65. W. Schakel, H. Meerman, A. Talaei, A. Ramírez and A. Faaij, *Applied Energy*, 2014, **131**, 441-467.
66. C. Wulf and M. Kaltschmitt, *Sustainability*, 2018, **10**, 1699.
67. M. Delpierre, J. Quist, J. Mertens, A. Prieur-Vernat and S. Cucurachi, *Journal of Cleaner Production*, 2021, **299**.
68. S. Fazio, V. Castellani, S. Sala, E. Schau, M. Secchi, L. Zampori and E. Diaconu, *Journal*, 2018.
69. P. Ruiz, A. Sgobbi, W. Nijs, C. Thiel, F. Dalla Longa, T. Kober, B. Elbersen and G. Hengeveld, *JRC Science for Policy Report, European Commission*, 2015.
70. P. Ruiz, W. Nijs, D. Tarvydas, A. Sgobbi, A. Zucker, R. Pilli, R. Jonsson, A. Camia, C. Thiel and C. Hoyer-Klick, *Energy Strategy Reviews*, 2019, **26**, 100379.
71. J. N. Van Stralen, A. Uslu, F. Dalla Longa and C. Panoutsou, *Biofuels, Bioproducts Biorefining*, 2013, **7**, 147-163.
72. S. Teske, *Achieving the Paris climate agreement goals: Global and regional 100% renewable energy scenarios with non-energy GHG pathways for+ 1.5 C and+ 2 C*, Springer Nature, 2019.
73. Eurostat, Electricity prices for non-household consumers - bi-annual data, <http://appsso.eurostat.ec.europa.eu/nui/submitViewTableAction.do>, (accessed 31. January, 2022).
74. Eurostat, Labour cost levels by NACE Rev. 2 activity, [https://ec.europa.eu/eurostat/databrowser/product/pag_e/LC_LCI_LEV\\$DEFAULTVIEW](https://ec.europa.eu/eurostat/databrowser/product/pag_e/LC_LCI_LEV$DEFAULTVIEW), (accessed 31. January, 2022).
75. J. Hengstler, M. Russ, A. Stoffregen, A. Hendrich, S. Weidner, M. Held and A. K. Briem, *Aktualisierung und Bewertung der Ökobilanzen von Windenergie- und Photovoltaikanlagen unter Berücksichtigung aktueller Technologieentwicklungen. Abschlussbericht*, 2021.
76. finanzen.net, Oil price (Brent), <https://www.finanzen.net/rohstoffe/oelpreis>, (accessed 1. November, 2022).
77. European Parliament Council of the European Union, *Directive (EU) 2018/2001 of the European Parliament and of the Council of 11 December 2018 on the promotion of the use of energy from renewable sources*, Official Journal of the European Union, 2018.
78. F. Habermeyer, J. Weyand, S. Maier, E. Kurkela and R.-U. Dietrich, *Biomass Conversion and Biorefinery*, 2023, DOI: 10.1007/s13399-022-03671-y.
79. B. Vidal-Legaz, S. Sala, A. Antón, D. M. De Souza, M. Nocita, B. Putman and R. F. Teixeira, *Joint Research Centre: Luxembourg*, 2016.
80. D. S. Lee, D. W. Fahey, P. M. Forster, P. J. Newton, R. C. N. Wit, L. L. Lim, B. Owen and R. Sausen, *Atmos Environ (1994)*, 2009, **43**, 3520-3537.
81. European Commission, Hydrogen: Commission supports industry commitment to boost by tenfold electrolyser manufacturing capacities in the EU https://ec.europa.eu/commission/presscorner/detail/en/p_22_2829, (accessed 8 December, 2022).
82. AsahiKasei, <https://www.asahi-kasei.com/news/2020/ze200403.html> (accessed 10 August 2021).

Journal Name

ARTICLE

83. European Commission, 'Fit for 55': delivering the EU's 2030 Climate Target on the way to climate neutrality, <https://eur-lex.europa.eu/legal-content/EN/TXT/?uri=CELEX%3A52021DC0550>, (accessed 15. March, 2023).
84. A. Liebich, T. Fröhlich, D. Münter, H. Fehrenbach, J. Giegrich, S. Köppen, F. Dünnebeil, W. Knörr, S. Simon and S. Maier, System comparison of storable energy carriers from renewable energies, <https://www.umweltbundesamt.de/publikationen/system-comparison-of-storable-energy-carriers-from>).

Supplementary Material

Sustainable aviation fuel from forestry residue and hydrogen – a techno-economic and environmental analysis for an immediate deployment of the PBtL process in Europe

Felix Habermeyer, Veatriki Papantoni, Ralph-Uwe Dietrich and Urte Brand-Daniels

Modelling Assumptions

Tab. 1. Modelling assumptions implemented in Aspen Plus®.

Unit	Description	Source
Dryer	Biomass moisture outlet: 15 wt-%, heat consumption: $1300 \text{ kWh}/t_{\text{H}_2\text{Oevap}}$, power consumption: $32 \text{ kWh}/t_{\text{drybio}}$, pressure: 1 bar	1
Gasifier	Heat loss = 1 % of input biomass LHV. $\Delta p = -0.2 \text{ bar}$. $T = 850^\circ\text{C}$, $p = 4.0 \text{ bar}$ ¹ Oxygen feed iterated to attain specified heat loss Minimum CO_2/O input = 1.0 (mass based) Feeding temperature = 200°C Modelled with RStoic and RGibbs. RGibbs (PR-BM) temperature 900°C Hydrocarbon formation (mol/kg of fuel volatiles): $\text{CH}_4 = 6.7826$, $\text{C}_2\text{H}_4 = 0.4743$, $\text{C}_2\text{H}_6 = 0.2265$, $\text{C}_6\text{H}_6 = 0.2764$ Tars modelled as naphthalene: $\text{C}_{10}\text{H}_8 = 0.0671$ Fuel nitrogen converted to NH_3 Fuel sulphur converted to H_2S Fuel ash to 100% to fly ash Fuel carbon: 0.05 % to fly ash All other components assumed to be in simultaneous phase and chemical equilibrium.	1
Filter	$\Delta p = -0.2 \text{ bar}$. Inlet temperature 550°C Complete removal of ash	1
Reformer	$T = 850^\circ\text{C}$ Adiabatic Oxygen feed iterated to attain specified heat loss Modelled as RGibbs Phase and chemical equilibrium conversion for C_{2+} and tar. CH_4 conversion: 35 % NH_3 conversion: 50 % $\Delta p = -0.2 \text{ bar}$	1
Water scrubber	Scrubbing liquid: water. $T_{\text{inlet}} = 200^\circ\text{C}$. Two-step cooling: $T_{1 \text{ out}} = 60^\circ\text{C}$, $T_{2 \text{ out}} = 30^\circ\text{C}$. Modelled as Flash using Soave-Redlich-Kwong (SRK) equation of state model.	1
Syngas compressor	$p_{\text{out}} = 25 \text{ bar}$ 5 stages with intercooling to 100°C Equal pressure ratio Isentropic efficiency 80 % Mechanical efficiency 100 %	1

Selexol scrubber	T = 0 °C 90 % removal of CO ₂ removal of ammonia (100%) and H ₂ S (90 %) Modelled as a separator block Energy consumption: 74 kJ/kg _{CO₂,removed} CO ₂ outlet pressure: 1 bar	2, 3
Guard bed	Complete removal of trace components Modelled as a separator block	4
FT reactor	220 °C, 25 bar, Slurry bubble column reactor Catalyst mass iterated to reach 55 % CO conversion Kinetic reaction model from ⁵ Products: n-alkanes and primary alkenes with a carbon chain length up to 30	5
Product separation	Tout = 0 °C Modelled with separator blocks Complete separation of Products C ₅₊ Recycle ratio 95 % of tail gas	
AEL	70.8 % HHV efficiency Modelled as a splitter p = 25 bar Hydrogen output iterated for a H ₂ /CO = 2.1 at FT inlet	6
CO ₂ Compressor	One stage compression Isentropic efficiency: 80 % Mechanical efficiency: 100 %	1

Tab. 2. FCI factors for equipment cost estimation methods.

Indirect cost factors	1	2	3	4	5
Source	7	8	1	1	
Installation factor	0.39	0.1	0	0	0
Instrumentation and control	0.26	0.36	0	0	0
Piping system	0.31	0.5	0	0	0
Electrical systems	0.1	0.1	0	0	0
Buildings	0.29	0.18	0	0	0
Yard improvements	0.12	0.1	0	0	0
Service facilities	0.55	0.4	0	0	0
Engineering and supervision	0.32	0.32	0.15	0.10	0

Construction cost	0.34	0.41	0	0	0
Legal expenditure	0.04	0.04	0	0	0
Contractor's fee	0.05	0.05	0	0	0
Contingency	0.1	0.1	0	0	0

Tab. 3. Indirect operating expenditure factors taken from [46].

	Factor [%]	Basis
Operating supervision (OS)	15	OL
Maintenance labour (ML)	1	FCI
Maintenance material (MM)	1	FCI
Operating supplies	15	ML + MM
Laboratory charges	20	OL
Insurances and taxes	2	FCI
Plant overhead costs (PO)	60	Total labour cost (OL + OS + ML)
Administrative costs	25	PO
Distribution and selling cost	6	NPC
Research and development4 costs		NPC

Mass balances

The stream data for selected process streams is presented in Tab. 4. The streams are numbered according to the order shown in Fig. 1.

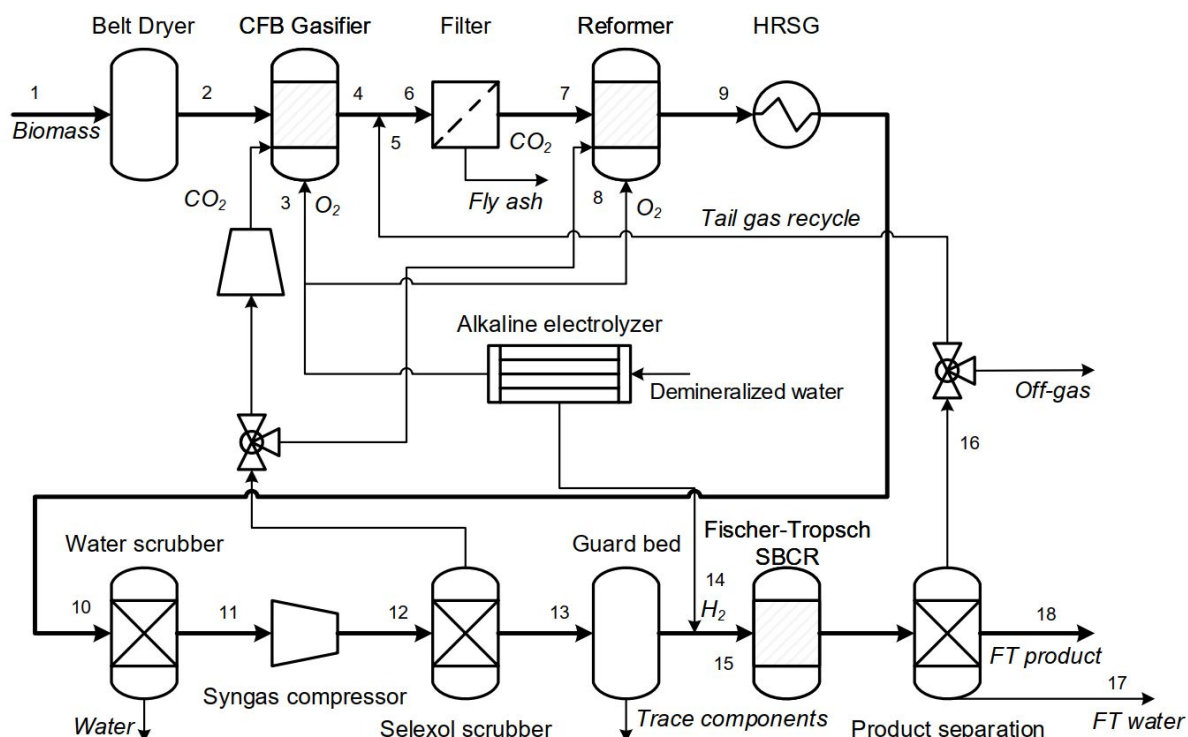


Fig. 1. Process flowsheet with stream numbers as referred to in Tab. 4.

Tab. 4. Stream data for selected process streams.

Stream number	1	2	3	4	5	6
	Wet biomass feed Dryer	Gasifier feed	Recycle and oxygen to Gasifier	Syngas from Gasifier	Recycle syngas	Filter feed
Temperature °C	25.0	65.5	199.9	850.0	0.0	600.0
Pressure bar	1	1	4	3.8	24.9	3.8
Molar flow kmol/s			0.4946	1.8158	3.2024	5.0182
Mass flow kg/s	47.3569	27.857	18.3523	46.2093	40.3801	86.5894
Composition						
H2 mol/mol				0.1901	0.5451	0.4167
CO mol/mol				0.3561	0.2831	0.3095
CO2 mol/mol			0.425	0.2399	0.0173	0.0979
H2O mol/mol				0.1386		0.0502
O2 mol/mol			0.575			
N2 mol/mol					0.0075	0.0048
CH4 mol/mol				0.0626	0.1383	0.1109
C2H6 mol/mol				0.0021	0.0016	0.0018
C3H8 mol/mol					0.0014	0.0009

C4H10	mol/mol			0.0013	0.0008	
C10H8	mol/mol				0.0002	
C6H6	mol/mol				0.0009	
NH3	mol/mol			0.0006	0.001	
H2S	mol/mol			0.0026	0.0001	
C2H4	mol/mol			0.0002	0.0017	
C3H6	mol/mol			0.0028	0.0025	0.0016
C4H8	mol/mol			0.0002	0.0017	0.0011

Other components

Biomass	kg/s	47.3569	27.857		
Fly ash	kg/s			0.9298	0.9298

Stream number		7	8	9	10	11
		Reformer feed	CO2 recycle and oxygen to Reformer	Syngas to HRSG	Syngas to Water Scrubber	Syngas to Compressor
Temperature	°C	600.0	199.8	900.0	60.0	30
Pressure	bar	3.6	3.6	3.4	3.4	3.4
Molar flow	kmol/s	5.0182	0.6217	5.9766	5.9764	5.2841
Mass flow	kg/s	85.6596	23.6827	109.3423	109.3415	96.869

Composition

H2	mol/mol	0.4167		0.3581	0.3581	0.405
CO	mol/mol	0.3095		0.3547	0.3547	0.4012
CO2	mol/mol	0.0979	0.5072	0.0977	0.0977	0.1105
H2O	mol/mol	0.0502		0.1242	0.1242	0.0095
O2	mol/mol		0.4928	0.	0.	
N2	mol/mol	0.0048		0.0042	0.0042	0.0048
CH4	mol/mol	0.1109		0.0605	0.0605	0.0685
C2H6	mol/mol	0.0018				
C3H8	mol/mol	0.0009				
C4H10	mol/mol	0.0008				
C10H8	mol/mol	0.0002				

C6H6	mol/mol	0.0009			
NH3	mol/mol	0.001	0.0004	0.0004	0.0005
H2S	mol/mol	0.0001	0.	0.	0.0001
C2H4	mol/mol	0.0017			
C3H6	mol/mol	0.0016			
C4H8	mol/mol	0.0011			

Stream number		12	13	14	15	16	17
		Syngas to Selexol Scrubber	Syngas to Guard Beds	Hydrogen from Electrolyzer	Syngas to Fischer-Tropsch Reactor	Fischer-Tropsch gas fraction	FT Water
Temperature	°C	0	0	60	220	0	25
Pressure	bar	25	25	25	25	24.9	24.9
Molar flow	kmol/s	5.2841	4.7055	2.2061	6.9115	3.3709	1.1658
Mass flow	kg/s	96.869	72.7807	4.4472	77.2269	42.5053	21.0028
Composition							
H2	mol/mol	0.405	0.4548	1.	0.6288	0.5451	
CO	mol/mol	0.4012	0.4505		0.3067	0.2831	
CO2	mol/mol	0.1105	0.0124		0.0084	0.0173	
H2O	mol/mol	0.0095					1.
O2	mol/mol						
N2	mol/mol	0.0048	0.0054		0.0037	0.0075	
CH4	mol/mol	0.0685	0.0769		0.0523	0.1383	
C2H6	mol/mol					0.0016	
C3H8	mol/mol					0.0014	
C4H10	mol/mol					0.0013	
C10H8	mol/mol						
C6H6	mol/mol						
NH3	mol/mol	0.0005					
H2S	mol/mol	0.0001	0.				
C2H4	mol/mol					0.0002	

C3H6 mol/mol 0.0025

Stream number 18

Fischer-Tropsch product

T [°C] °C 10.3

Pressure bar 24.9

Molar flow kmol/s 0.0795

Mass flow kg/s 13.7188

Composition

C5H12	mol/mol	0.0555	C24H50	0.0216	C17H34	0.0011
C6H14	mol/mol	0.0515	C25H52	0.0207	C18H36	0.0008
C7H16	mol/mol	0.0482	C26H54	0.0198	C19H38	0.0006
C8H18	mol/mol	0.0453	C27H56	0.019	C20H40	0.0004
C9H20	mol/mol	0.0428	C28H58	0.0182	C21H42	0.0003
C10H22	mol/mol	0.0406	C29H60	0.0174	C22H44	0.0002
C11H24	mol/mol	0.0386	C30H62	0.0167	C23H46	0.0002
C12H26	mol/mol	0.0367	C5H10	0.0558	C24H48	0.0001
C13H28	mol/mol	0.035	C6H12	0.0395	C25H50	0.0001
C14H30	mol/mol	0.0335	C7H14	0.0281	C26H52	0.0001
C15H32	mol/mol	0.032	C8H16	0.0201	C27H54	0.
C16H34	mol/mol	0.0306	C9H18	0.0145	C28H56	0.
C17H36	mol/mol	0.0292	C10H20	0.0104	C29H58	0.
C18H38	mol/mol	0.028	C11H22	0.0075	C30H60	0.
C19H40	mol/mol	0.0268	C12H24	0.0055		
C20H42	mol/mol	0.0257	C13H26	0.004		
C21H44	mol/mol	0.0246	C14H28	0.0029		
C22H46	mol/mol	0.0235	C15H30	0.0021		
C23H48	mol/mol	0.0225	C16H32	0.0015		

Cost estimation

Tab. 5. Utility cost and revenue form by-products.

Utility/Raw material	Quantity per hour	Market price (2020)	Total costs per year [€/a]	
Electricity	943.6(MWh)	50.4(€/MWh)	385201017.2	
Cooling Water	38535.1(m ³)	0.005(€/m ³)	1560670.61	
Biomass	170.5(t)	42.232(€/t)	58,319,311	
Demineralized water	153.9(m ³)	2.032(€/m ³)	2,533,575	
Cobalt catalyst	7.9(kg)	32.918(€/kg)	2,094,963	
Selexol	0.0034(t)	4394.808(€/t)	121,389	
Stack maintenance	16010.0(kg)	0.109(€/kg)	14,135,217	
Waste Water	126.5(m ³)	0.918(€/m ³)	1,059,734	
Total costs:			465,339,078	
By-products	Quantity per hour	Market price (2020)	Total revenue per year [€/a]	
Low Pressure Steam	-319.95(t)	13.142(€/t)	-	34,058,741
Medium Pressure Steam	-109.3392(t)	16.057(€/t)	-	14,220,842
High pressure steam	-195.8112(t)	17.706(€/t)	-	28,082,968
Total revenue:			-	76,362,552

Tab. 6. Equipment cost and fixed capital investment cost for all process units.

	Equipment cost [M€]	Fixed capital investment [M€]
Dryer	37.64	37.64
AEL Stack	686.43	686.43
AEL BoP	60.87	247.12
Filter	19.52	29.18
Guard Bed	31.74	38.41

Selexol	24.24	103.70
Striper	16.94	24.12
CFB gasifier	58.78	71.13
HRSO	20.32	30.37
Refrigeration System	6.97	29.81
CO ₂ Compressor	2.42	3.45
Syngas Compressor	16.37	23.32
Reformer	50.20	71.50
FT SBCR Vessel	13.99	59.85
FT SBCR Catalyst	18.14	77.59
Cold Trap	0.09	0.38
Total	1,064.66	1,534.00

Tab. 7. Annuity calculation.

Fixed Capital Investment [FCI]	1,534.00	M€
Working capital	10.00%	of TCI
Total Capital Investment [TCI]	1,704.44	M€
Operating time of plant	20	years
Interest rate	7.00%	
Annuity factor	0.094392926	
Annuity	156.73	M€/year

Tab. 8. Net production cost calculation (NPC).

Direct production costs	Cost per year [M€/a]
Operating labour [OL]	3.45
Operating supervision	0.52
Maintenance labour	15.34

Maintenance material	15.34
Operating supplies	4.60
Laboratory charges	0.69
Raw materials and utilities	464.91
Revenue from by-products	- 76.36
Indirect production costs	-
Insurances and taxes	30.68
Plant overhead costs	11.59
General expenses	-
Administrative costs	2.90
Annuity	156.73
	630.38
Indirect production costs	Cost per year [M€/a]
Distribution and selling costs	42.03
Research and development costs	28.02
Production cost	700.42
Product output per year [Mt/a]	0.40
Net production cost [€/kg]	1.75

Local economic/ecologic analysis

Tab. 9. National economic/ecologic conditions relevant for the PBTl production.

NUTSO	Electricity price [€/MWh]⁹	Carbon intensity [gCO₂eq/kWh]¹⁰	Labour cost [€/h]¹¹	Transport Cost [€/t/km]¹²
FR	53.5	51.1	37.5	0.48
AL	51.6	-	2.6 ^a	0.18
AT	73.6	82.4	36.7	0.45
BA	62.7	-	5.2 ^a	0.19
BE	41.8	161.0	41.1	0.47
BG	57.9	410.4	6.5	0.22
CY	114 ^a	620.9	17	0.36
CZ	63.2 ^a	436.6	14.1	0.29
DE	64.3	311.0	36.6	0.45
DK	47.1	109.0	45.8	0.68
EE	68.8 ^a	774.9	13.6	0.28

EL	59.7 ^a	479.2	16.9	0.37
ES	50.3	156.4	22.8	0.41
FI	45.9	68.6	34.3	0.49
HR	58.4	133.8	10.8	0.26
HU	65.6	216.4	9.9	0.24
IE	78.6	278.6	32.3	0.44
IT	57.8	213.4	29.8	0.45
LT	63.2 ^a	45.4	10.1	0.24
LU	47.3 ^a	58.5	42.1	0.48
LV	69.5 ^a	106.5	10.5	0.26
ME	56.9	-	5.6 ^a	0.2
MK	53.4	-	3.6 ^a	0.17
MT	86 ^a	379.0	14.5	0.3
NL	59.5	328.4	36.8	0.5
NO	30.8	19 ^d	47.3	0.53 ^c
PL	75.3	709.8	11	0.27
PT	69.8	198.4	15.7	0.29
RO	67.5	299.5	8.1	0.21
RS	58.3	-	5.8 ^a	0.19
SE	35.6	8.8	37.3	0.53
SI	65.2 ^a	217.8	19.9	0.32
SK	94.4	101.7	13.4	0.27
UK	136.1	225.0	28.5 ^a	0.48

a data from past years used instead of 2020S1.

b Electricity price from 70 – 150 GWh consumer category.

c Assumed same transport cost as Sweden

d Value from 2019 used ¹³

GHG Abatement cost calculation

Tab. 10. Assumptions for the GHG abatement calculation.

	<i>Value</i>	<i>Unit</i>
Oil price (Brent)¹⁴	75.06	\$/barrel
Volumetric conversion¹³	158.98	l/barrel
Currency conversion¹⁵	0.877	€/€
Oil price	0.415	€/l

Impact categories for LCA

Tab. 11. Impact categories used in the LCA.

Impact category	Indicator	Unit	Abbreviation
Climate change	Radiative forcing as Global Warming Potential (GWP100)	kg CO ₂ eq	GWP
Ozone depletion	Ozone Depletion Potential (ODP)	kg CFC-11eq	ODP
Particulate matter/ Respiratory inorganics	Human health effects associated with exposure to PM2.5	Disease incidences	PM
Photochemical ozone formation	Tropospheric ozone concentration increase	kg NMVOC eq	POF
Acidification	Accumulated Exceedance (AE)	mol H+ eq	AP
Eutrophication, terrestrial	Accumulated Exceedance (AE)	mol N eq	TEP
Eutrophication, aquatic freshwater	Fraction of nutrients reaching freshwater end compartment (P)	kg P eq	FEP
Eutrophication, aquatic marine	Fraction of nutrients reaching marine end compartment (N)	kg N eq	MEP
Ecotoxicity (freshwater)	Comparative Toxic Unit for ecosystems (CTUe)	CTUe	FETP
Land use	Soil quality index (Biotic production, Erosion resistance, Mechanical filtration and Groundwater replenishment)	Dimensionless, aggregated index	LU
Water scarcity	User deprivation potential (deprivation-weighted water consumption)	kg world eq. deprived	WS
Resource use, minerals and metals	Abiotic resource depletion (ADP ultimate reserves)	kg Sb eq	MM
Resource use, energy carriers	Abiotic resource depletion – fossil fuels (ADP-fossil)	MJ	ECF

Economic allocation

Tab. 12. Economic allocation factors for the LCA.

Flow	Quantity [t/h]	Price [€/t]	Revenue [€/h]	Allocation factor
FT product	49.39	1,750.00	86,428.27	0.9016
Low Pressure Steam	319.95	13.14	4,204.78	0.0439
Medium Pressure Steam	109.34	16.06	1,755.66	0.0183
High pressure steam	195.81	17.71	3,467.03	0.0362
Total	-	-	95,855.74	1

Life Cycle Inventories

The following tables contain the data used to model the PBtL processes as part of the LCA. The names and locations of the process flows correspond to the ones used in the ecoinvent v3.7.1 database. In the processes that include electricity as an input (i.e. Selexol production and PBtL production) the electricity entry was adapted to correspond to the respective scenario (e.g. Swedish grid). For the sake of simplicity only one such case is shown here. The amounts shown here correspond to the base case as described in Section 6. Flows with no entry in the column "Location" are biosphere flows. Tab. 13 to Tab. 21 list the LCIs for the processes that make up the LCI of the entire PBtL production process shown in Fig. 1.

Tab. 13. LCI of the production of 1 kg of Selexol taken from ¹⁶.

Selexol production flows	Amount	Unit	Location
market for ethylene oxide	7.50E-01	kg	RER
market for methanol	0.2	kg	GLO
market for water, decarbonised	0.05	kg	DE
market for natural gas, high pressure	0.05	cubic meter	DE
steam production, in chemical industry	0.5	kg	RER
market for electricity, medium voltage	3.00E-01	kilowatt hour	EE
Water, cooling, unspecified natural origin	2.50E-02	cubic meter	
Methanol	1.00E-04	kg	
Ethylene oxide	1.00E-04	kg	

Tab. 14. LCI for the production of 1 kg of cobalt catalyst based on ⁵.

Cobalt catalyst production flows	Amount	Unit	Location
market for cobalt	0.25	kg	GLO
market for molybdenum	0.0356	kg	GLO
market for aluminium oxide, non-metallurgical	0.7452	kg	IAI Area, EU27 & EFTA
market for process-specific burdens, residual material landfill	1	kg	Europe without Switzerland

Tab. 15. LCI for the production of 1 kg of nickel catalyst based on the data acquired in the FLEXCHX project.

Nickel catalyst production flows	Amount	Unit	Location
market for nickel, class 1	0.15	kg	GLO
market for aluminium oxide, non-metallurgical	0.85	kg	IAI Area, EU27 & EFTA
market for process-specific burdens, residual material landfill	1	kg	Europe without Switzerland

Tab. 16. LCI for the production of 1 kg of guard bed material.

Guard bed material production flows	Amount	Unit	Location
--	---------------	-------------	-----------------

market for activated carbon, granular	1	kg	GLO
market for process-specific burdens, residual material landfill	1	kg	Europe without Switzerland

Tab. 17. LCI for the provision of 1 kg of forest residue biomass. This inventory is based in the ecoinvent activity "market for wood chips, wet, measured as dry mass, Europe without Switzerland", but adapted to not include the biomass coming from sawmills, in order to only describe primary residues. The transport activities contained in the original ecoinvent process were omitted here and explicitly included in the PBtL-production LCI as a separate flow.

Forest residue biomass flows	Amount	Unit	Location
hardwood forestry, birch, sustainable forest management	0.399	kg	SE
softwood forestry, spruce, sustainable forest management	0.1709	kg	SE
softwood forestry, pine, sustainable forest management	0.157	kg	SE
hardwood forestry, beech, sustainable forest management	0.137	kg	DE
softwood forestry, spruce, sustainable forest management	0.068	kg	DE
softwood forestry, pine, sustainable forest management	0.042	kg	DE
hardwood forestry, oak, sustainable forest management	0.027	kg	DE

Tab. 18. LCI for the construction of a PBtL plant corresponding to the base case of a 400 MW plant. The assumed lifetime is 20 years. This is a combination of data from ecoinvent processes for a syngas plant and a refinery plant each scaled to the capacity of the PBtL plant, and data from literature for the electrolysis plant (also scaled up to the modelled electrolyzer capacity)¹⁷. The output of this process is one unit of PBtL plant.

PBtL plant construction flows	Amount	Unit	Location
synthetic gas factory construction	1.00E+02	unit	CH
petroleum refinery construction	4.00E-01	unit	RER
market for steel, low-alloyed	2.82E+07	kg	GLO
market for aluminium, cast alloy	7.04E+04	kg	GLO
market for chromium	1.53E+05	kg	GLO
market for nickel, class 1	3.13E+05	kg	GLO
market for polyethylene, high density, granulate	5.54E+04	kg	GLO

Tab. 19. LCI of the emissions and associated waste treatment processes from the production of 1 MJ of FT product as derived from the Aspen Plus model. The output of this process is one unit of emissions.

Emission flows	Amount	Unit	Location
market for wood ash mixture, pure	-1.54E-03	kg	Europe without Switzerland
Hydrogen (to air)	2.20E-09	kg	
Carbon monoxide, from soil or biomass stock (to air)	8.89E-09	kg	
Carbon dioxide, from soil or biomass stock (to air)	5.74E-03	kg	
Nitrogen (to water)	1.024E-10	kg	
Nitrogen (to air)	5.887E-05	kg	

Methane, from soil or biomass stock (to air)	6.06E-09	kg
Ammonia (to air)	7.168E-05	kg
Hydrogen sulfide (to water)	1.671E-05	kg

Tab. 20. LCI of other commodities needed for the production of 1 MJ of FT product as derived from the Aspen Plus model. The output of this process is one unit of other commodities.

Other commodity flows	Amount	Unit	Location
market for water, deionised	7.10E-02	kg	Europe without Switzerland
market for potassium hydroxide	1.48E-05	kg	GLO
Water, cooling, unspecified natural origin	1.78E-02	cubic meter	

Tab. 21. LCI of the modelled PBtL plant for the production of 1 MJ of FT product. The LCI includes the flows as listed in the tables above. Amounts in this LCI have been scaled with the economic allocation factor as presented in section 6.5.

PBtL production flows	Amount	Unit	Location
Forest residue biomass	4.17E-02	kg	Europe without Switzerland
transport, freight, lorry 16-32 metric ton, EURO6	7.09E-03	ton kilometer	RER
market for electricity, medium voltage	3.92E-01	kilowatt hour	SE
Other commodities	9.02E-01	unit	GLO
Selexol production	1.42E-06	kg	RER
Cobalt catalyst production	3.27E-06	kg	RER
Nickel catalyst production	2.74E-06	kg	RER
Guard bed material production	2.00E-06	kg	RER
Emissions	9.02E-01	unit	GLO
PBtL plant construction	2.566E-12	unit	RER

Additional visualisations

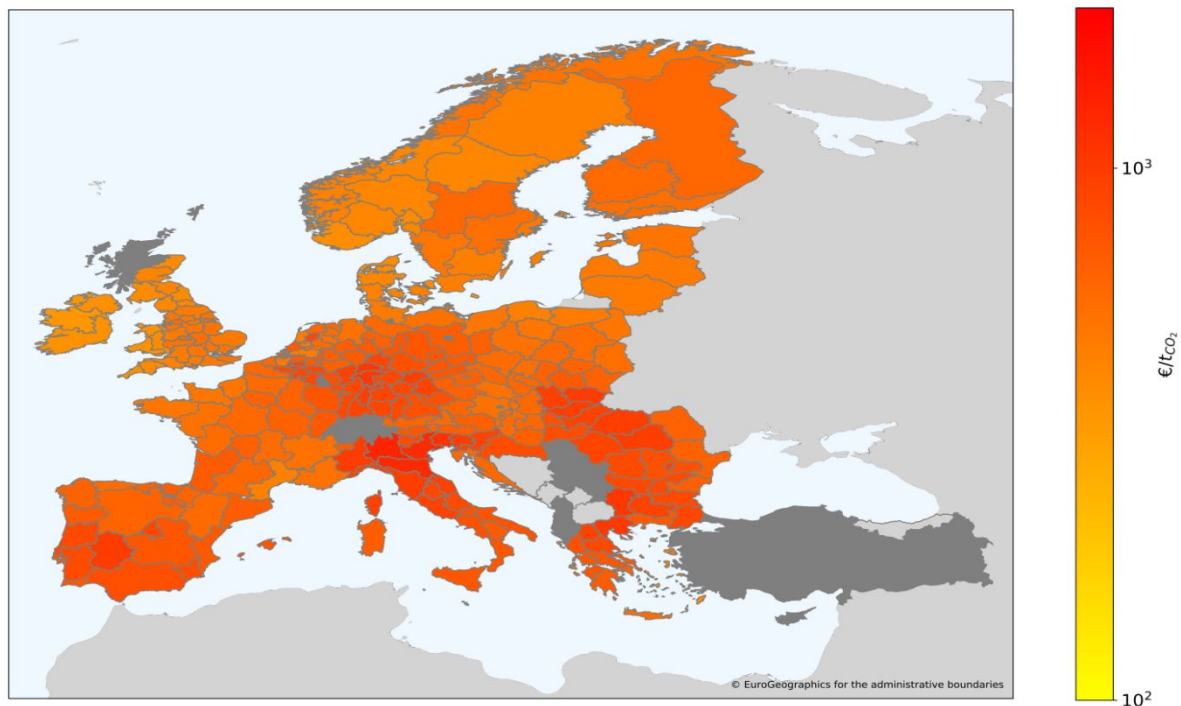


Fig. 2. Abatement cost [$\text{€}_{2020}/\text{t}_{\text{CO}_2}$] for wind park connected PBtL production in the hydrogen storage scenario.

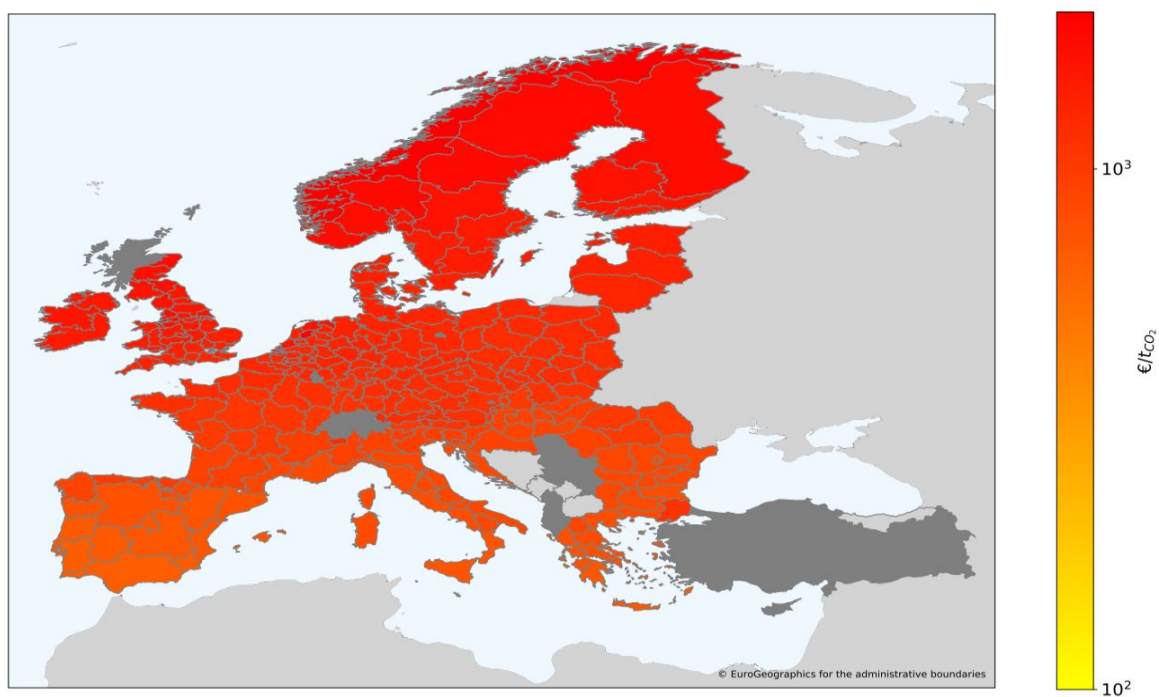


Fig. 3. Abatement cost [$\text{€}_{2020}/\text{t}_{\text{CO}_2}$] for PV connected PBtL production in 2020 in the hydrogen storage scenario.

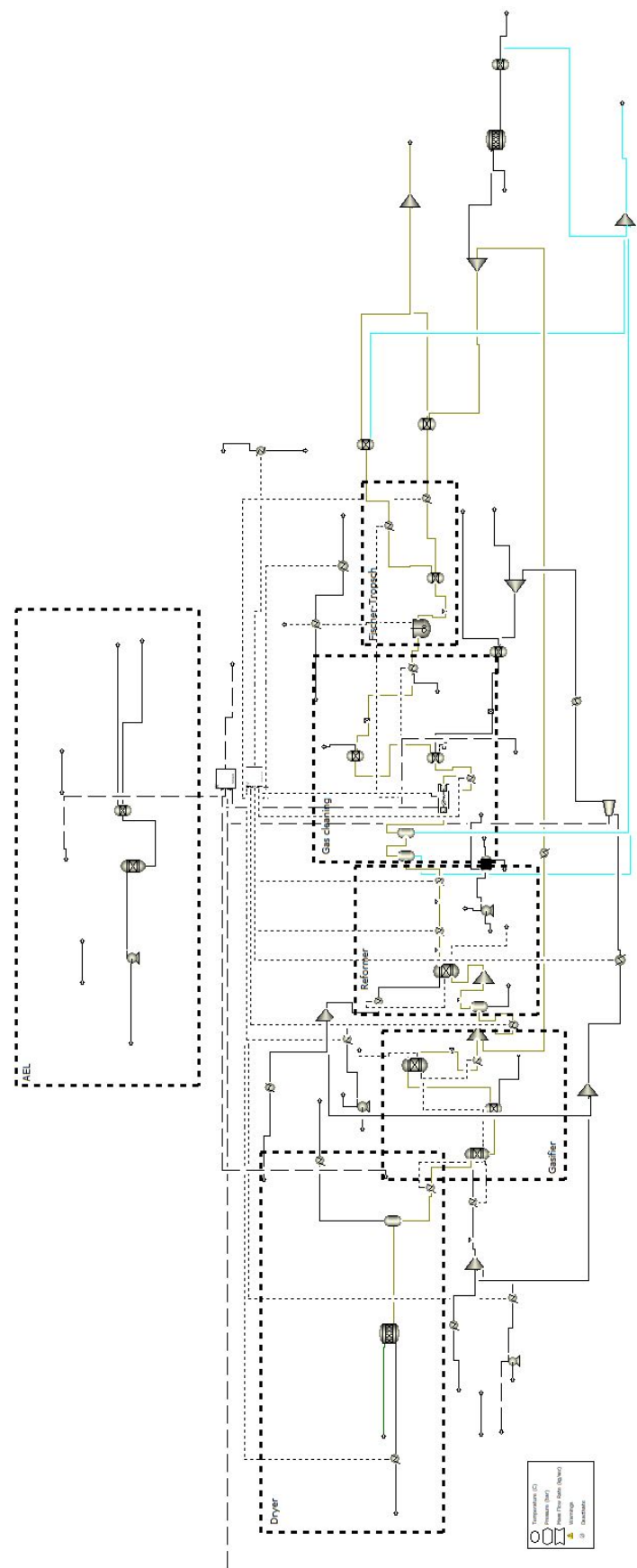
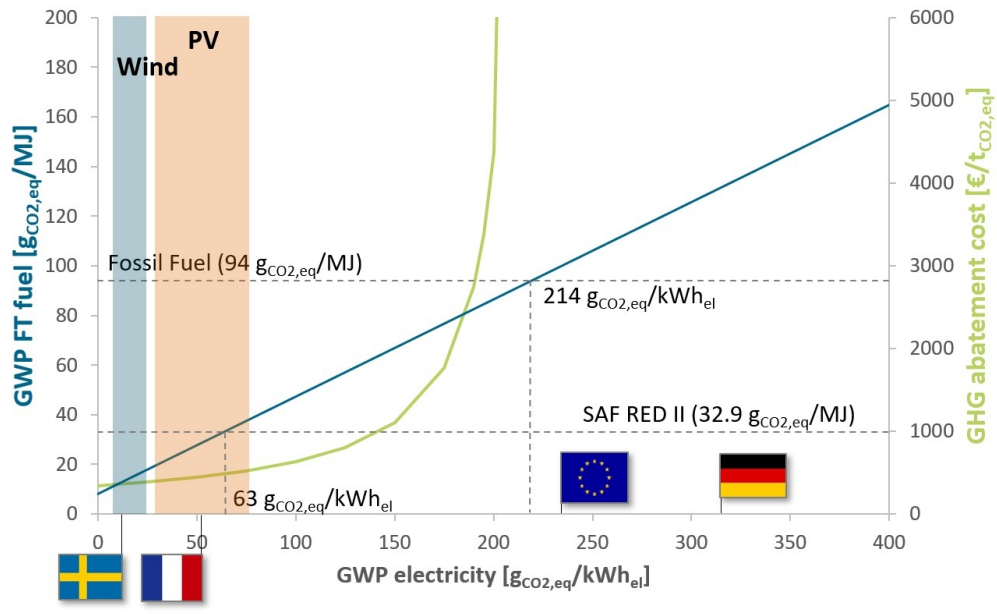


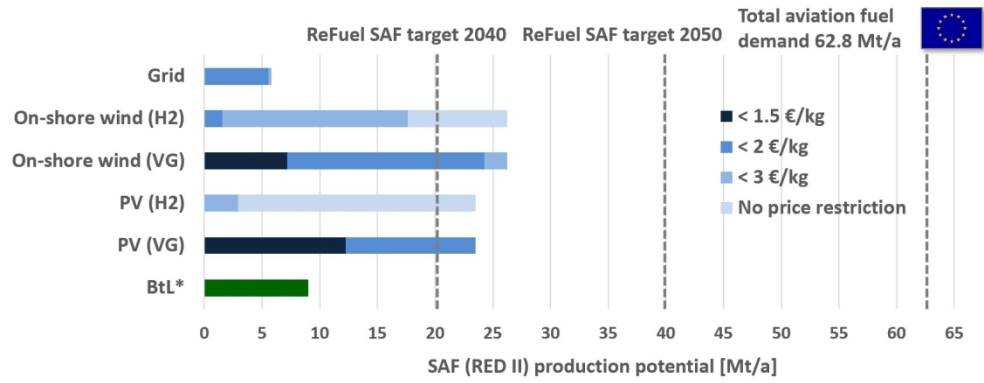
Fig. 4 Aspen Plus flowsheet of the PBtL process

References

1. I. Hannula, *Energy*, 2016, **104**, 199-212.
2. M. Hillestad, M. Ostadi, G. A. Serrano, E. Rytter, B. Austbø, J. Pharoah and O. S. Burheim, *Fuel*, 2018, **234**, 1431-1451.
3. C. N. Hamelinck and A. P. Faaij, *Energy policy*, 2006, **34**, 3268-3283.
4. C. Frilund, E. Kurkela and I. Hiltunen, *Biomass Conversion and Biorefinery*, 2021, DOI: 10.1007/s13399-021-01680-x.
5. B. Todici, T. Bhatelia, G. F. Froment, W. Ma, G. Jacobs, B. H. Davis and D. B. Bukur, *Industrial Engineering Chemistry Research*, 2013, **52**, 669-679.
6. A. Buttler and H. Spliethoff, *Renewable and Sustainable Energy Reviews*, 2018, **82**, 2440-2454.
7. M. S. Peters, K. D. Timmerhaus and R. E. West, *Plant design and economics for chemical engineers*, McGraw-Hill New York, 2003.
8. F. Habermeyer, E. Kurkela, S. Maier and R.-U. Dietrich, *Frontiers in Energy Research*, 2021, **9**, 684.
9. Eurostat, Electricity prices for non-household consumers - bi-annual data, <http://appsso.eurostat.ec.europa.eu/nui/submitViewTableAction.do>, (accessed 31. January, 2022).
10. European Environmental Agency, Greenhouse gas emission intensity of electricity generation by country https://www.eea.europa.eu/data-and-maps/daviz/co2-emission-intensity-9/#tab-googlechartid_googlechartid_googlechartid_chart_1111, (accessed 31. January, 2022).
11. Eurostat, Labour cost levels by NACE Rev. 2 activity, [https://ec.europa.eu/eurostat/databrowser/product/page/LC_LCI_LEV\\$DEFAULTVIEW](https://ec.europa.eu/eurostat/databrowser/product/page/LC_LCI_LEV$DEFAULTVIEW), (accessed 31. January, 2022).
12. P. Ruiz, A. Sgobbi, W. Nijs, C. Thiel, F. Dalla Longa, T. Kober, B. Elbersen and G. Hengeveld, *JRC Science for Policy Report, European Commission*, 2015.
13. I. Staffell, The Energy and Fuel Data Sheet, https://www.claverton-energy.com/wordpress/wp-content/uploads/2012/08/the_energy_and_fuel_data_sheet1.pdf, (accessed 11, 2021).
14. finanzen.net, Oil price (Brent), <https://www.finanzen.net/rohstoffe/oelpreis>, (accessed 1. November, 2022).
15. ExchangeRates.org.uk, US Dollar to Euro Spot Exchange Rates for 2020, <https://www.exchangerates.org.uk/USD-EUR-spot-exchange-rates-history-2020.html>, (accessed 22.11., 2022).
16. W. Schakel, H. Meerman, A. Talaei, A. Ramírez and A. Faaij, *Applied Energy*, 2014, **131**, 441-467.
17. C. Wulf and M. Kaltschmitt, *Sustainability*, 2018, **10**, 1699.



339x210mm (96 x 96 DPI)



451x173mm (96 x 96 DPI)